Photo-activated drug delivery systems

Kong, L.

1

The Application of Sheddable PEG Coronas in Drug Delivery

Abstract: To prolong *in vivo* circulation times of drug delivery nano-systems, poly(ethylene glycol) (PEG) is often used to sterically shield nanoparticle surfaces. This serves to minimize adsorption of serum proteins to the nanoparticle and recognition and bodily clearance *via* the mononuclear phagocyte system (MPS). However, a PEG corona also inhibits interactions between nano-carriers and target cells, limiting drug delivery and effective therapy. To overcome this dilemma, cleavable PEG coronas have been developed to maintain long circulation lifetimes of nanoparticles while also achieving efficient cellular interactions with targeted cells. In this chapter, various strategies and examples of drug delivery systems with a sheddable PEG corona are reviewed.

1.1 Introduction

In the treatment of cancer, the challenge is how to deliver cytotoxic drugs to cancer cells while minimizing off-target toxicity in healthy cells and tissue. Current chemotherapy is characterized by debilitating side effects[1] (impaired immune system, nausea, cardiomyopathy, hair loss) and in many cases, the cumulative lifetime dose of an anti-cancer drug must be limited to avoid permanent damage.[2] Intense efforts have therefore been made to develop drug delivery systems (DDS) capable of delivering drugs specifically to cancer cells (Figure 1).[3]

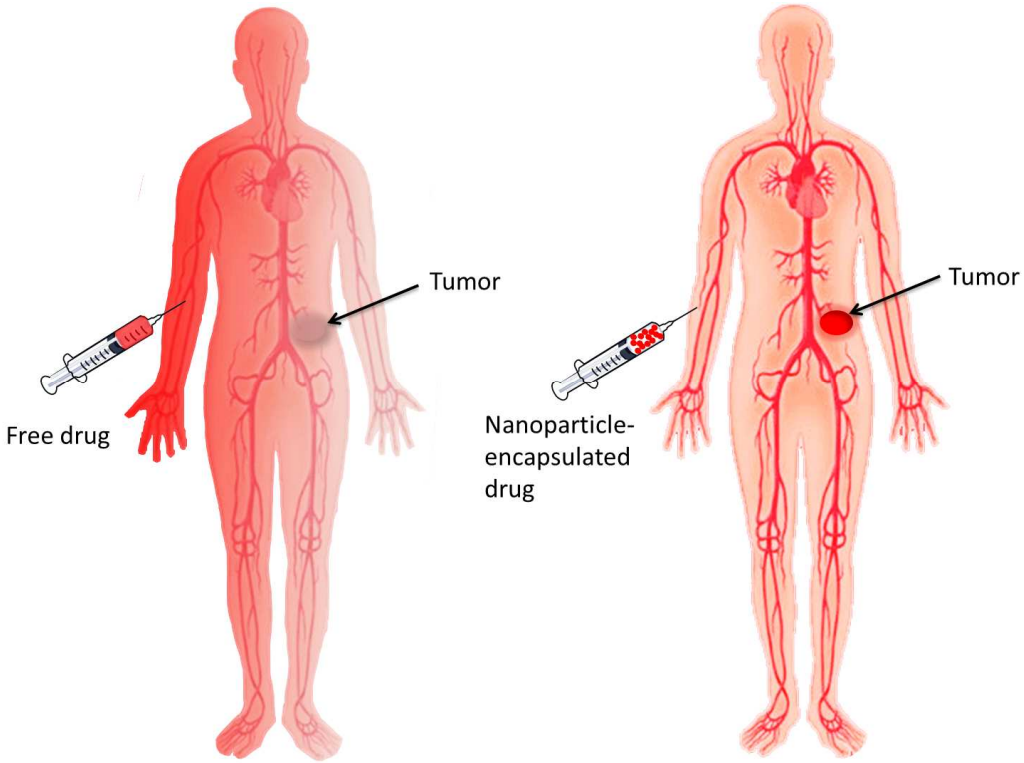

Figure 1. Distribution of free (left) and nanoparticle-encapsulated (right) drugs within the body following systemic (*e.g.* intravenous) administration. Small molecule drugs freely diffuse through tissue and away from the site of injection (non-targeted). Nanoparticles remain restricted within blood vessels and can passively accumulate within tumors (targeted). Image taken from www.cocoavia.com.

Two principle technologies have emerged: antibody-drug conjugates (ADCs) and nanoparticle-based systems. Currently, 5 ADCs and 12 distinct nanoparticle-based

DDS targeted against a variety of human cancers are on the market.[4] For ADCs, 'active' targeting is achieved through antibody recognition and binding to over-expressed receptors (tumor-associated antigens) on cancer cells.[5] Once bound, ADCs are endocytosed, the conjugated drug released and ideally the cell is destroyed. Although effective, ADCs are costly to manufacture, can elicit adverse immunogenic responses (limiting repeat dosing) and are largely limited to small molecule drug (and serum stable) cargos.[6] In the case of nanoparticle-based DDS, drugs are encapsulated within the structure of the self-assembled nanoparticle, hidden and protected from the *in vivo* environment. Pharmacokinetic (PK) profiles are dictated by the nanoparticle and, in theory, it is possible to deliver anything from small molecule drugs to plasmid DNA to target cells and tissue within the body. An enormous variety of nanoparticle-based DDS have been reported, however the most widely investigated are micelles, liposomes and polymersomes (Figure 2).[7] In the treatment of cancer, the vast majority of nanoparticle-based systems 'passively' target tumors *via* the enhanced permeability and retention (EPR) effect.

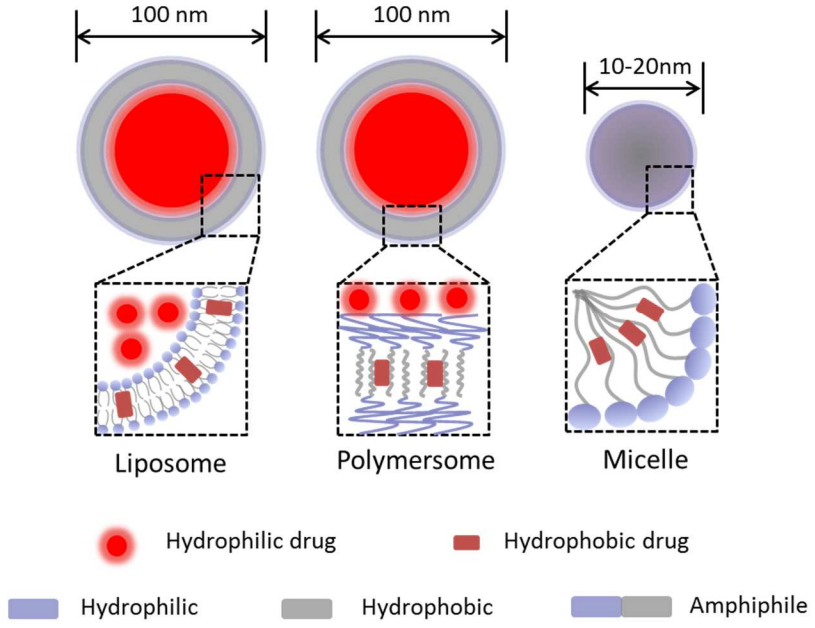

Figure 2. Schematic showing the three most commonly self-assembled nanoparticle- based drug delivery systems. Self-assembly is primarily driven by the burial of hydrophobic functionality of amphiphilic building blocks to limit exposure to water ('hydrophobic effect').

1.1.1 The enhanced permeability and retention (EPR) effect

Following administration to the body, small molecule drugs freely diffuse away from the site of injection (Figure 1). In contrast, following intravenous (*i.v.*) injection, nanoparticles are restricted to the circulating blood flow, unable to cross the tightly packed endothelium due to their larger size. For optimal biodistribution, nanoparticles should be larger than 10 nm in diameter – below which they are filtered from the body *via* the kidneys – and smaller than 200 nm in diameter – above which they are recognized and phagocytosed by macrophages (key cells of the mononuclear phagocyte system, MPS) and cleared from the body.[8]

The EPR effect is a phenomena characterized by the ill-defined ('leaky') vasculature and poor lymphatic drainage of tumors arising from rapid angiogenesis (blood vessel growth) within tumor tissue (Figure 3).[9] Circulating nanoparticles passing through a tumor can passively diffuse across gaps in the tumor endothelium, accumulate within the tumor and remain there for extended periods of time. Once within the tumor, nanoparticle encapsulated drugs can either passively diffuse from the nanoparticle or an endogenous or exogenous stimulus can trigger release.

A key difference between the various strategies described in this chapter is whether the nanoparticle is internalized prior to drug release or not. If it is first internalized, drug release occurs intracellular and beyond the barrier of the cell membrane. This offers opportunities to deliver membrane impermeable cargos such as DNA, RNA and proteins to cancer cells. If extracellular drug release occurs, the drug must be taken up by cancer cells itself. In either scenario, it is essential cancer cells are exposed to therapeutically relevant doses of cytotoxic drugs if an improved therapeutic index is to be achieved.

There are several nanoparticle-based DDS (*e.g*. Doxil®), currently on the market, designed to passively target chemotherapies to solid tumors *via* the EPR effect.[10] These have been clinically proven to improve patient quality of life compared to administration of the free drug alone. Nevertheless, the effectiveness of this targeting approach remains contentious.[11] A recent analysis (>200 separate studies) of nanoparticle uptake in tumors *via* the EPR revealed, for instance, found, on average,

just 0.7% of the injected nanoparticle dose accumulated within the target tumor.[12] In addition, there is growing evidence that the EPR effect may be more pronounced in experimental animal models than in human patients,[13] therefore running the risk of false positives entering clinical evaluation. Finally, it is becoming increasingly clear that there is significant physiological heterogeneity within and between tumor types in patients. In other words, the same nanoparticle-based DDS may give very different therapeutic outcomes in two patients suffering from the same cancer.[14] In light of this, there are growing calls for pre-selection of patients to effectively identify those who would likely benefit from these technologies over those who would likely not.[15]

1.1.2 Polyethylene glycol (PEG)

To maximize nanoparticle targeting of tumors *via* the EPR effect, nanoparticles with long circulation lifetimes are sought. Put simply, the more times nanoparticles pass through the tumor vasculature, the more will accumulate there. As such, care must be taken to minimize drug leakage from the nanoparticle *en route* to the tumor while at the same time ensuring therapeutically relevant concentrations of drugs are released once there. In the case of liposome-drug formulations – the most widely investigated and major class of nanoparticles approved for clinical use[16] – this involves careful choice of lipid reagents (*e.g.* cholesterol to rigidify fluid, leaky membranes) to fine tune drug retention/release profiles while at the same time maximizing circulation lifetimes.[17]

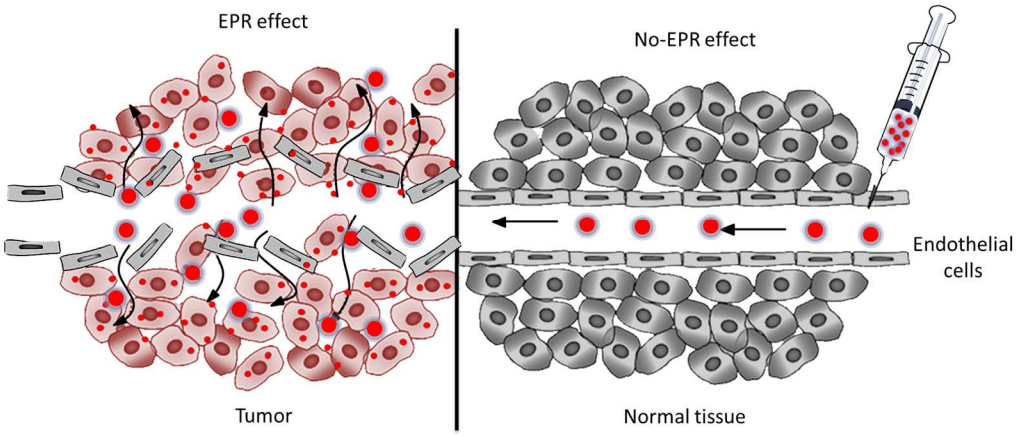

Figure 3. Schematic representation of the EPR effect. Healthy cells are shown in grey and tumor cells in red. The small red dots indicate drug release from the nanoparticle and delivery to cells once nanoparticles have accumulated within the target tumor. Image taken from[18].

In developing nanoparticles with long circulation lifetimes, the principle biological barrier to overcome is recognition and clearance of nanoparticles by the MPS. The principle organ of the MPS is the liver where hepatic macrophages – Kupffer cells – are highly proficient at recognizing and removing macromolecular, colloidal and pathogenic waste from circulation.[19] Without any surface modification, up to 99% of nanoparticles are cleared through the liver.[20] In most cases, it is believed rapid adsorption of blood proteins to the surface of nanoparticles, (a process known as opsonisation), acts as a recognition beacon for the MPS.[21] For this reason, sterically shielding nanoparticle surfaces with biocompatible polymers such as polyethylene glycol (PEG), has been used to minimize opsonisation and prolong blood circulation times of nanoparticles *in vivo*.[22]

a

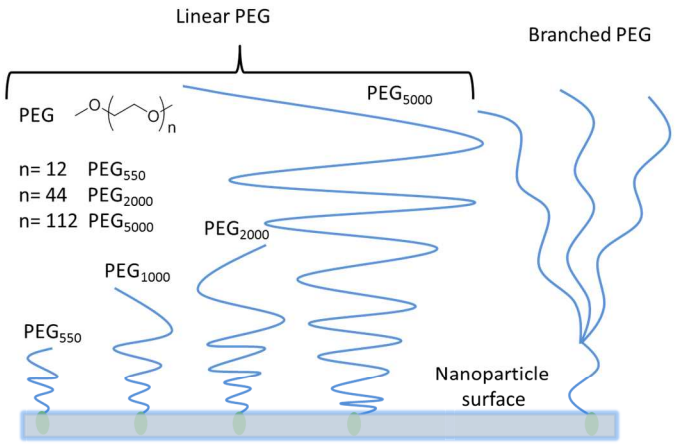

b

Therapeutic type	Commercial name	Drug name	PEG (g/mol)	Indications
Enzyme	Adagen	PEGademase bovine	5000 (linear)	severe combined immunodeficiency disease
	Oncaspar	PEGaspargase	5000 (linear)	lymphoblastic leukemia
Interferons	PegIntron	peginterferon-2β	12000 (linear)	hepatitis B and hepatitis C
	Puricase	PEG-urate oxidase	10000	Gout
	Pegasys	peginterferon-2α	40000 (branched)	hepatitis C
Granulocyte colony stimulating factor	Neulasta	pegfilgrastim	20000 (linear)	neutropenia
Growth hormone receptor antagonist	Somavert	pegvisomant	5000 (linear)	Acromegaly
Drug	Macugen	Pegaptanib sodium	40000 (branched)	age-related macular degeneration(AMD)
	Movanti	pegylated naloxol	339	Opoid-induced constipation
Erythropoietin receptor activator	Mircera	Mono-mPEG-epoetin-β	30000 (linear)	Anemia associated with chronic renal failure
Antibody	Cimzia	certolizumab pegol	40000 (branched)	Reducing signs and symptoms of Crohn's disease

Figure 4. (a) The chemical structure and representation of linear PEG chains with different lengths and branched PEG; (b) Table of FDA approved PEGylated drugs.[23]

PEG is a synthetic polymer of repeating ethylene glycol units. Used as a reagent or additive in a wide range of biological, chemical and industrial settings,[24] it is commercially available in a range of geometries (linear, branched, star, comb), molecular weights (from 300 Da – 6-7 repeating units – up to 10 MDa - >200,000 repeating units) and can be readily functionalized. PEGylation of nanoparticle surfaces

has been shown to decrease serum protein adsorption, reduce nanoparticle uptake in the liver and prolong circulation lifetimes.[25] More recently, evidence has been uncovered to suggest PEG can elicit an immunogenic response.[26] However, the extent and accuracy of the immunogenic response caused by binding of anti-PEG antibodies to PEGylated nanoparticles remains unclear.[27] PEG remains an FDA approved polymer and is still the most widely used polymeric coating of nanoparticle DDS both in academic and industrial research.

Numerous PEGylated products, such as PEGylated enzymes, proteins, antibodies or oligonucleotides, are FDA-approved (Figure 4). For example, PEGylated liposomal-doxorubicin (Doxil®) has been clinically used for over 20 years in the treatment of select breast and ovarian cancers, multiple myeloma and AIDS-related Kaposi's sarcoma.[24b]

1.1.3 The PEG dilemma

While PEGylation serves to prolong circulation lifetimes, it also limits the cellular uptake of nanoparticles. This has proved a major obstacle in the targeted delivery of therapeutic cargos, particularly those that must be actively transported across the target cellular membrane.[28] For instance, in the delivery of oligonucleotides (ODNs) or small interfering RNAs (siRNAs), significantly lower transfection/transduction efficiencies were observed for PEGylated vs. non-PEGylated DDS.[29] To overcome this 'PEG dilemma', many strategies have been proposed to trigger the shedding of PEG (*i.e.* dePEGylation) from a nanoparticle surface upon reaching the target tumor. In the vast majority of cases, triggered dePEGylation within the target tumor occurs outside of the target cell (extracellular). This leads to one of three scenarios: 1) rupture of the nanoparticle and extracellular drug release (Figure 5a); 2) cellular uptake of the intact nanoparticle-drug complex (Figure 5b) or 3) in the case of liposomal carriers, fusion of the nanoparticle with the target cellular membrane resulting in contents release directly to the cell cytoplasm (*i.e.* avoiding endocytotic uptake) (Figure 5c). In a small number of examples, PEGylated nanoparticles used to be taken up by the cancer cells first whereupon the low pH, reductive and protease-rich environment of the late endosome/lysosome triggers dePEGylation and contents release (Figure 5d).

However, the slow rate of uptake of PEGylated nanoparticles is a major obstacle to these approaches.

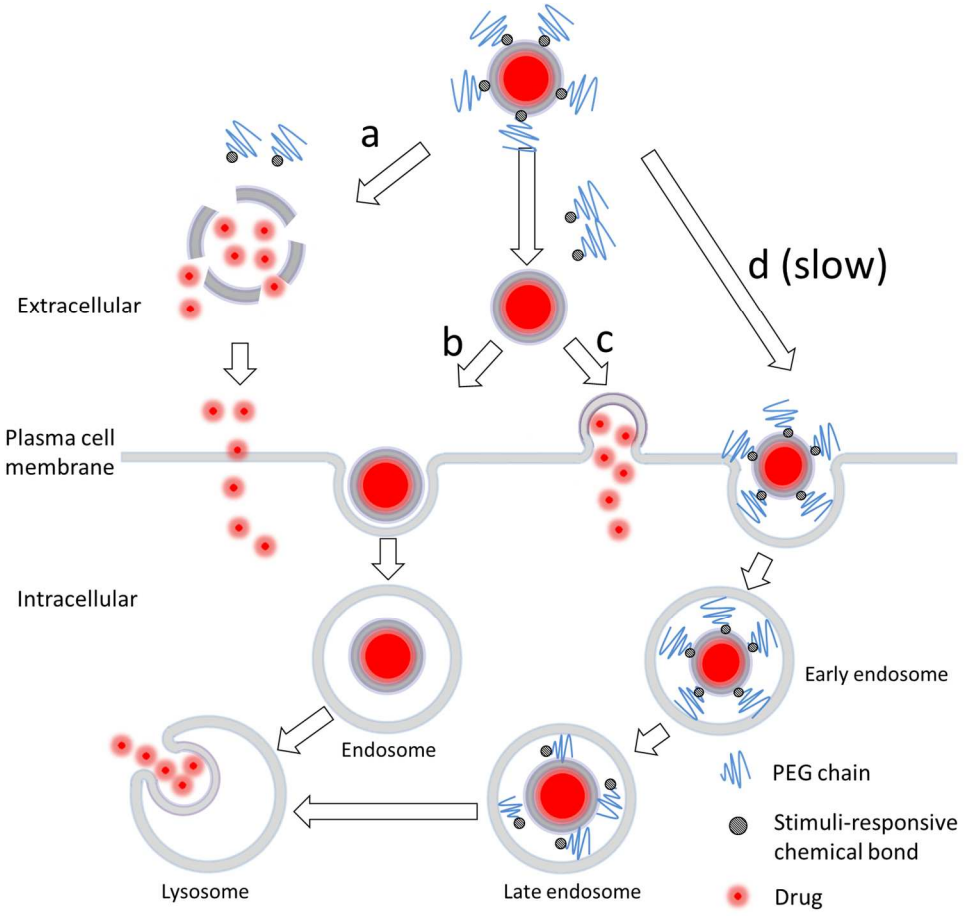

Figure 5. Schematic illustration of the various drug release outcomes following dePEGylation of a nanoparticle: (a) extracellular dePEGylation, nanoparticle rupture and extracellular drug release; (b) extracellular dePEGylation followed by endocytotic uptake and intracellular drug release; (c) extracellular dePEGylation followed by nanoparticle fusion with the plasma cell membrane and drug delivery direct to the cell cytosol; and (d) intracellular dePEGylation following endocytotic uptake of PEGylated nanoparticle and intracellular drug release.

1.2 Physical dePEGylation strategies

Two principal physical approaches to achieve dePEGylation of nanoparticle surfaces have been investigated. The first, most relevant for liposome DDS, relies on the

exchange of PEGylated lipids from a drug carrier (*e.g.* liposome) surface to a target membrane sink (*e.g.* target cancer cell membranes).[30] Here, the rate at which exchange occurs is heavily dependent on the structure of the lipid anchoring PEG to the liposome membrane (*i.e.* how strongly it is embedded within the liposome membrane).[31] In a study of three different lipid-PEG conjugates, no lipid-PEG exchange was observed for long chain, saturated lipid anchors (DSPE-PEG, C18:0) whereas exchange occurred in the time frame of hours for shorter saturated lipids (DMPE-PEG; C14:0) or long chain, unsaturated lipids (DOPE-PEG; C18:1).[32] This time frame enabled efficient accumulation of liposomes in tumor sites *via* the EPR effect (prior to dePEGylation) coupled with increased cellular uptake within the tumor (following dePEGylation). Conversely, a similar study found that only in the case of DSPE-PEG where circulation times was improved to achieve efficient passive accumulation of nanoparticles within the tumor.[33] These conflicting results highlight the fine balance required to achieve efficient accumulation and subsequent dePEGylation within the tumor microenvironment. The propensity for non-specific PEG exchange with biological membranes *in vivo,* prior to reaching the target tumor, has likely limited the widespread application of this approach.

The second physical approach relies on non-covalent adsorption of PEG onto a nanoparticle surface, for example, carboxylate-functionalized PEG adsorbed to a cationic nanoparticle surface.[34] In this case, protonation of carboxylate groups within the acidic tumor microenvironment can be expected to lead to dePEGylation. While this approach is conceptually simple, the stability of the absorbed PEG corona in serum and the propensity of premature dePEGylation under physiological conditions (*e.g.* high salt) and/or through competition from other serum components has likewise limited the widespread investigation of this approach.

1.3 Chemical dePEGylation strategies

The most common method to dePEGylate nanoparticle surfaces is through chemical approaches. In these cases, PEG is connected to the nanoparticle *via* a stimuli-responsive covalent chemical bond.[35] Stimuli can be both endogenous and exogenous. In the case of endogenous stimuli, intrinsic differences between pathological and healthy tissues are exploited, such as the lower pH and reducing

environments within the tumor microenvironment. Exogenous stimuli, including light and heat, have the benefit of being under complete user control in both time and space,[36] however these approaches rely on the ability to accurately deliver external stimuli to tissues often deep within the body. In next section, stimuli-responsive chemical bonds commonly used in the dePEGylation of nanoparticles are highlighted.

1.4 Stimuli-responsive bonds towards responsive dePEGylation

1.4.1 pH-sensitive dePEGylation

Both the acidic intracellular environment of endosomes (pH 5.0-6.5) and lysosomes (pH 4.5-5.0) and the mildly acidic (pH <7) extracellular environment within tumors have been exploited to trigger the release of PEG from nanoparticles. The most common pH-sensitive bonds used in these DDS are summarized in Table 1.

Table 1. pH sensitive bonds used in PEGylated DDS.

Name	Structure and hydrolysis process	Conjugated polymers	Features
β-thiopropionate	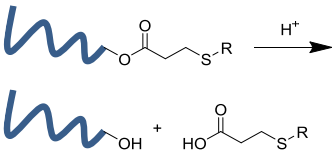	Oligodeoxynucleotide[37] or polymer[38]	Modify nucleotides; cleaved under endosomal acid conditions
Phosphoramidate	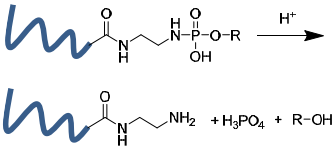	Oligodeoxynucleotide[39] or peptide[40]	Modify nucleotides; high yield and chemoselectivity
Hydrazone	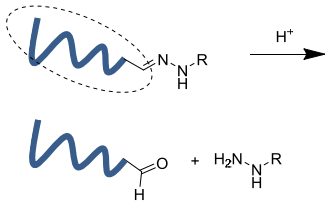	Lipid[41], drug[42]or polymer[43]	Controllable sensitivity, predictable pH-sensitivity
Ortho ester	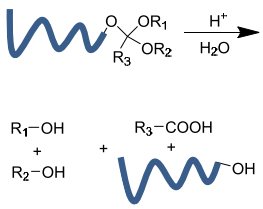	Alkyl[44], lipid[45] or polymer[46]	Controllable sensitivity, predictable pH-sensitivity
Vinylether	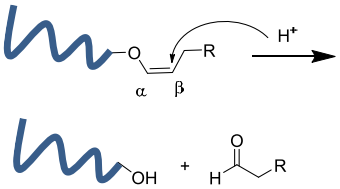	Lipid[47]	Controllable sensitivity, predictable pH-sensitivity
Imine bond	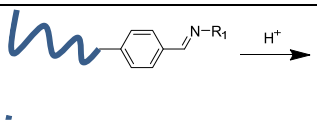	Lipid[48], Alkyl[49] drug[50] or nanoparticles[51]	Extracellular dePEGylation, charge shielding

Aconitic anhydride amide	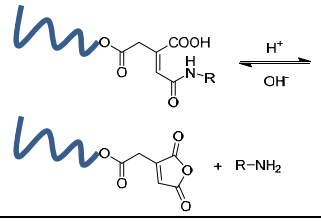	Doxorubicin[52]	Mild synthesis

In several cases, it has been shown possible to fine tune the sensitivity of acid hydrolysis to achieve optimal dePEGylation either within the tumor microenvironment or within endosomes. Walker *et al.* linked polycations (PEI or PLL) to PEG *via* acyl hydrazides or 2-pyridyl hydrazines (compound **1**, **2** and **3**; Figure 6a) and found that while compound **1** and **3** resulted in efficient dePEGylation at endosomal pH (pH=5), hydrolysis of **2** was extremely slow.[43a] Alternatively, it has been shown that the acid-catalyzed hydrolysis of pH-sensitive ortho esters is heavily affected by its substitution at positions R_1, R_2 and R_3 (Table 1), where methyl or 6-membrered cyclic esters increased the rate of acid catalyzed hydrolysis by at least an order of magnitude.[45b] At pH 4.0, compound **4** could be completely hydrolyzed while only 30% of **5** was degraded within 30 min (Figure 6b).

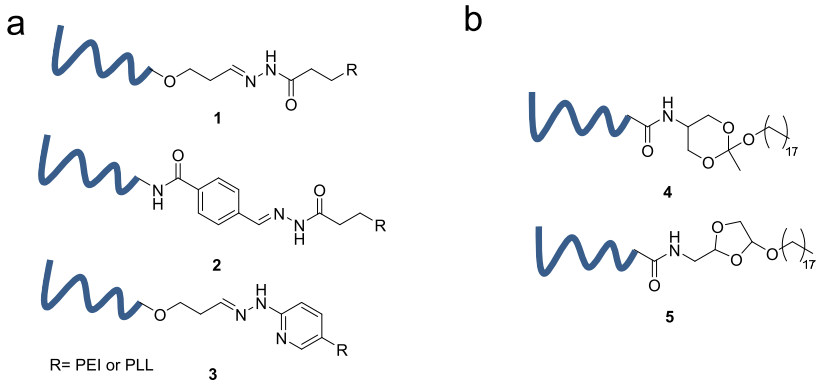

Figure 6. Substitutions of hydrazone (a) and ortho ester bond (b) fine-tune the pH-sensitivity.

1.4.2 Redox-sensitive dePEGylation

Glutathione (GSH), is an abundant reducing agent in most mammalian cells[53] and has been exploited to trigger redox-sensitive dePEGylation of DDS (Figure 7a). The intracellular concentration of GSH can span the range 2–10 mM, three orders of magnitude greater than the extracellular concentration of GSH (2–20 μM)[54] (Figure

7a). Furthermore, the concentration of GSH within the tumor microenvironment is 4 times higher than in normal tissue. Reduced GSH can cleave disulfide (S-S) bonds linking PEG to a nanoparticle surface through a process of disulfide exchange (Figure 7b). PEG-disulfide conjugates can be synthesized through disulfide exchange or through the use of symmetrical/asymmetrical disulfide-containing crosslinkers (Table 2). A variety of symmetrical and asymmetrical disulfide containing crosslinking reagents, such aldrithiol, cystamine, 2-hydroxyethyl disulfide, 3,3'dithiodipropionic acid, DTSP and SPDP have been used to generate redox-sensitive PEGylated DDS (Table 2).

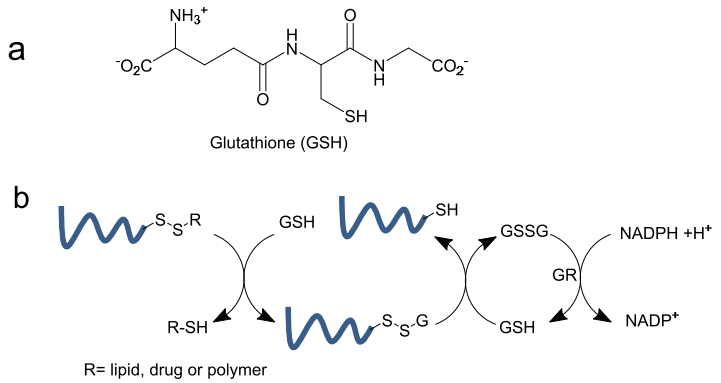

Figure 7. (a) The structure of GSH; (b) GSH mediated reduction of disulfide bonds.

Table 2. Methods and reagents for synthesizing PEGylated compounds containing disulfide bonds.

Crosslinker	Synthesis
Thiol-disulfide exchange	 R= lipid or polymer Aldrithiol[55]
Symmetrical crosslinker	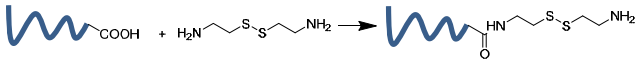 Cystamine[56]
	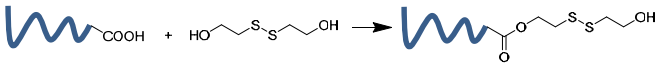 2-Hydroxyethyl disulfide[57]
	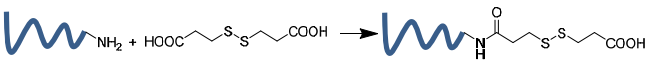 3,3'-dithiodipropionic acid[58]
	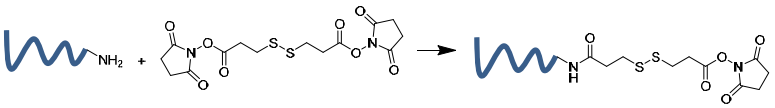 DTSP[59]
Asymmetrical crosslinker	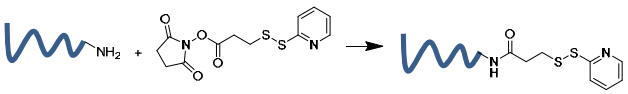 SPDP[60]

The first example of a redox sensitive PEGylated nanoparticle incorporated $mPEG_{2000}$-DTP-DSPE within a fusogenic liposome formulation, facilitating rapid and complete content release (Figure 8).[59] Partial cleavage of grafted PEG from liposomes by thiolytic agents successfully led to destabilization of liposome bilayers and complete contents release within 2 h. However, this system required high concentrations of thiolated agents (10 mM, 1,4-dithiothreitol) limiting its application *in vivo*. To overcome this, a new generation of reductive cleavable PEG-lipid (mPEG-DTB-DSPE) has been shown to undergo complete thiolytic cleavage at greatly reduced thiol concentrations (cysteine, 150 µM).[61] Moreover, cleavage of

mPEG-DTB-DSPE liberated unmodified DSPE (*i.e.* leaving no remnant thiol attached) which was essential to the recovery of fusogenicity of the DDS (Figure 8).

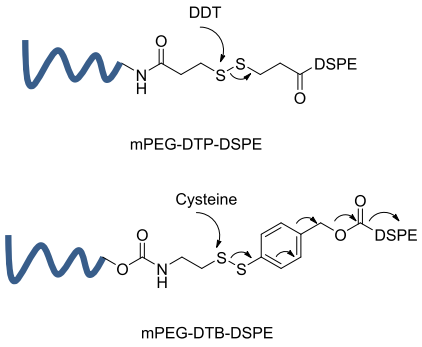

Figure 8. The structure of mPEG-DTP-DSPE and mPEG-DTB-DSPE and their thiolytic cleavage mechanisms.

1.4.3 Enzyme-sensitive dePEGylation

Within the tumor microenvironment, there are high levels of lytic enzymes. These are secreted by tumor cells to degrade the extracellular matrix (ECM) and aid cancer cell migration.[62] Short peptides containing enzyme-consensus sequences can therefore be used to enzymatically cleave PEG from a nanoparticle surface (Table 3). Two principle proteases have been exploited, matrix metalloproteinases (MMPs) and cathepsin B.

MMPs play an essential role in tumor invasion and metastasis by degrading a variety of extracellular proteins and ECM components.[63] MMPs, particularly MMP2 and MMP9, are highly expressed within, and secreted by, cancer cells. MMP-sensitive linkers have been employed to achieve tumor-specific and extracellular dePEGylation of various DDS including liposomes,[64] nanoparticles[65] and micelles.[66]

Cathepsin B is an intracellular cysteine protease found abundantly in endosomes and lysosomes. It is highly up-regulated in cancer cells[67] and cleaves peptides containing one of a variety of short recognition sequences. Cathepsin B-sensitive peptide linkers have been used to achieve endo/lysosomal dePEGylation, however the slow cellular uptake of PEGylated nanoparticles has limited the widespread application of cathepsin B-sensitive linkers.

Table 3. MMP2 and cathepsin B peptide recognition sequences (↓ represents position of enzymatic cleavage)

Enzyme	Peptide Sequences	Cleavage Site
MMP2-sensitive peptides[64-66, 68]	GPLG ↓ IAGQ; GGGPQG ↓ IWGQGK; GPL ↓ GIAG; GPL ↓ GV; PLG ↓ LAG	Extracellular
Cat B-sensitive peptides[69]	A↓A; A↓L; F↓R; F↓K; AF↓K; GL↓FG; GF↓LG	Intracellular

1.4.4 Light-sensitive bonds

Photolabile chemical bonds have been widely used in both chemistry and biology to precisely control where and when new functionality is revealed.[70] Unlike endogenous stimuli, such as pH, redox and enzymatic cleavage, the application of light can be precisely controlled in both time, space and intensity (*i.e.* is user defined) and requires no other reactive species (other than, in some cases, water). Light-based therapies have already entered the clinic. For example, photodynamic therapy[71] combines chemical photosensitizers and light to trigger the local production of cytotoxic singlet oxygen in the body and is used in the clinic to treat a wide range of medical conditions, including acne, atherosclerosis and cancer.[72]

Various photolabile bonds used to dePEGylated nanoparticle surfaces are summarized in Table 4. The vast majority of these are sensitive to high-energy UV light (<400 nm), wavelengths that not only demonstrate poor tissue penetration (100-200 μm) but also yields significant light-induced cytotoxicity.[73] Therefore several strategies have been developed to alleviate these issues. These include the use of fibre optic light sources to deliver UV light deep within tissue,[74] the development of photolabile chemical bonds sensitive to longer wavelength light[75] and increasing the efficiency of photolysis so as to minimize light exposure. One attractive option is to improve the sensitivity of photolabile bonds to two photon light.[76] Two-photon excitation requires two light sources perpendicular to one another, each delivering photons at twice the wavelength required (*e.g.* 365 nm vs 2 x 730 nm light) for photolysis. Only at the exact point of intersection is enough energy delivered to cleave the photolabile

bond. The use of longer wavelength light not only increases tissue penetration (>1 cm for near-IR light) and reduces the risk of light induced cytotoxicity but, by restricting light activation to the focal point of two photon beams, it provides exquisite spatial control over light activation. We and others have previously shown that o-nitrobenzyl groups, the most commonly used photolabile chemical bond, can be efficiently cleaved using 2-photon light.[77]

The work in this thesis primarily concerns the use of the *o*-nitrobenzyl (*o*-Nb) photolabile functionality. Non-hydrolytic photolysis of *o*-Nb proceeds through a cyclic intermediate followed by the release of the desired alcohol and a nitroso by-product (Scheme 1a).[78] *O*-Nb groups can also be used to 'photocage' primary amines, through the inclusion of a carbamate linker, producing CO_2 as a photolytic by-product (Scheme 1b). To broaden application in biological areas, modifications, such as substituting R_1 with methoxy groups, have been included to reduce the toxicity of the nitroso photolysis byproduct.

Table 4. Common light-cleavable bonds used in PEGylated DDS.

Photo-responsive group	Active wavelength	Photo-irradiated dePEGylation
Nitrobenzyl ester[38, 79]	300-400 nm	
2-nitrophenylalanine [80]	365 nm	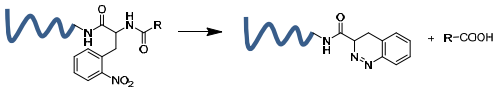
Truxillic acid[81]	< 260 nm	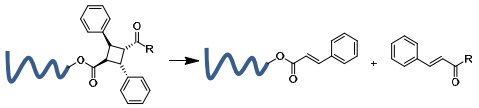
Trithiocarbonate[82]	232-500 nm	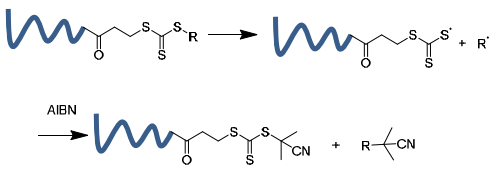
azobenzene[83]	280–450 nm	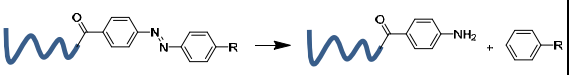
Boron dipyrromethene[84]	470-490 nm	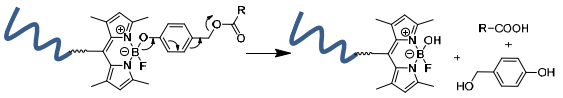
Fullerene[85]	350–700 nm	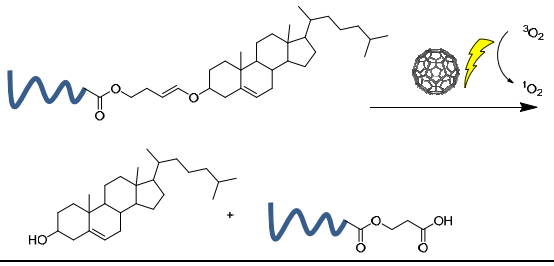
Platinum (IV)–azide complexes[86]	360-500 nm	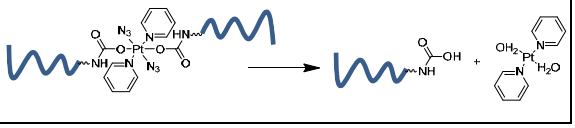

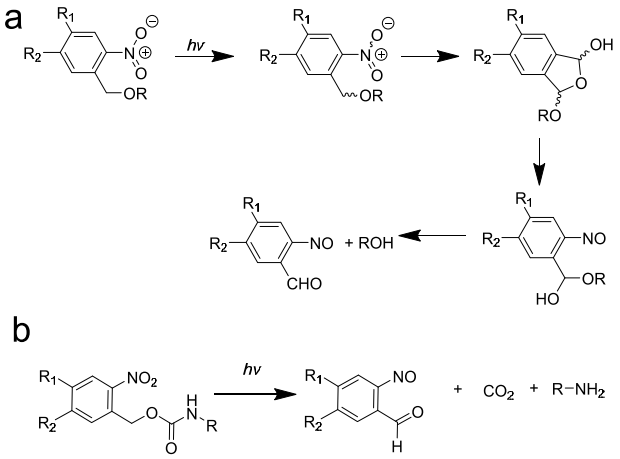

Scheme 1. The mechanism of cleavage of *o*-Nb substituted with ester (a) and carbamate (b).

1.5 DePEGylation of various drug carriers

1.5.1 Liposomes

Liposomes are formed through the self-assembly of amphiphilic (phospho)lipids in aqueous solution, forming closed spherical particles consisting of a lipid bilayer surrounding an inner aqueous core.[87] Within these structures, hydrophilic cargos/drugs can be encapsulated within the aqueous interior and hydrophobic cargos/drugs within the hydrophobic membrane. In both cases, cargos are protected from the outside environment. Self-assembly of liposomes is driven by the burial of hydrophobic fatty acid chains ('the hydrophobic effect') and each individual liposome comprises many thousands of individual lipid molecules (approximately 80,000 per 100 nm uni-lamellar liposome). The huge diversity of lipid reagents – both natural and non-natural – means the overall physicochemical properties of the liposome (size, surface charge, rigidity, surface functionalization) can be infinitely fine-tuned for a particular purpose. A selection of common lipids described and/or used throughout this thesis is shown in Table 5.

Table 5. the structure of lipids used in this thesis.

Name	Structure	Charge
(d18:1/12:0) Sphingomyelin	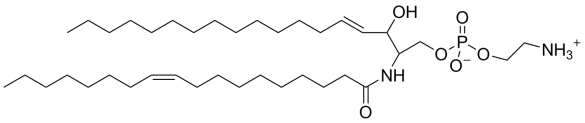	Zwitterionic
18:0 PC (DSPC)	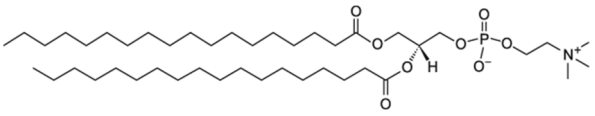	
18:1 (Δ9-Cis) PE (DOPE)	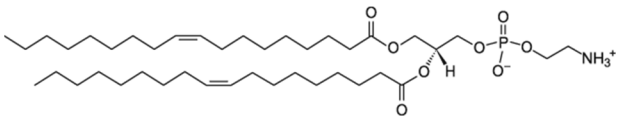	
18:1 (Δ9-Cis) PC (DOPC)	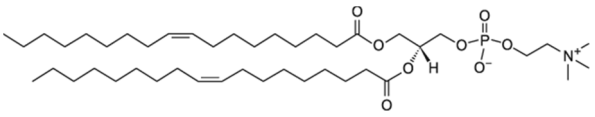	
Cholesterol	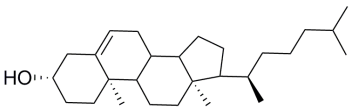	Neutral
18:1 TAP (DOTAP)	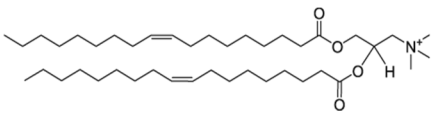	Cationic
18:1 (Δ9-Cis) PG (DOPG)	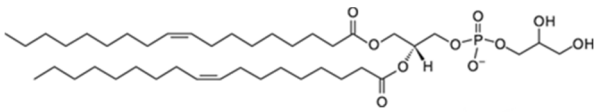	Anionic

1.5.1(a) Lipid geometries

Lipid packing within a liposome membrane is heavily influenced by the molecular geometries of individual lipid molecules. Based on the difference between the surface area of the hydrophilic head group and the volume of the hydrophobic fatty acid tail, amphiphilic lipids can be divided into three distinct molecular geometries: cylinder, cone and inverted-cone (Figure 9). The principle lipid components of biological membranes (and those most commonly found in reported liposome membranes) are cylinder shaped. Cylindrical lipids, with equal cross-sectional areas of both hydrophilic

head group and hydrophobic fatty acid tails, pack favorably to form lipid bilayers. Examples include phosphatidyl choline (PC), serine (PS) and glycerol (PG). Lipids such as sphingomyelin (SM), with a larger hydrophilic headgroup and a smaller hydrophobic volume, preferentially form micellar structures.[88] These smaller self-assembled structures (typically 10-20 nm in diameter) are characterized by a packed hydrophobic core and have no inner aqueous volume. Finally, inverted cone lipids, such as DOPE, do not form stable self-assembled structures in aqueous solution. These lipids preferentially pack into membranes demonstrating negative curvature and form inverted micelles in organic solutions. Although lipid membranes with negative curvature are rare, a key intermediate structure during the fusion of two lipid membranes (*e.g.* during SNARE-mediated fusion) requires lipids which favor negative curvature.[89]

Liposome membranes can comprise mixtures of different lipids and lipid geometries, so while it is not possible to make stable lipid bilayers using 100% DOPE, this lipid can be efficiently incorporated in stable lipid bilayers formed from cylinder-shaped lipids (eg, PC lipids). In all cases, the key driving force determining self-assembly, stability and structure of lipid mixtures in aqueous solution is the efficient burial of the hydrophobic core so as to minimize exposure to water.

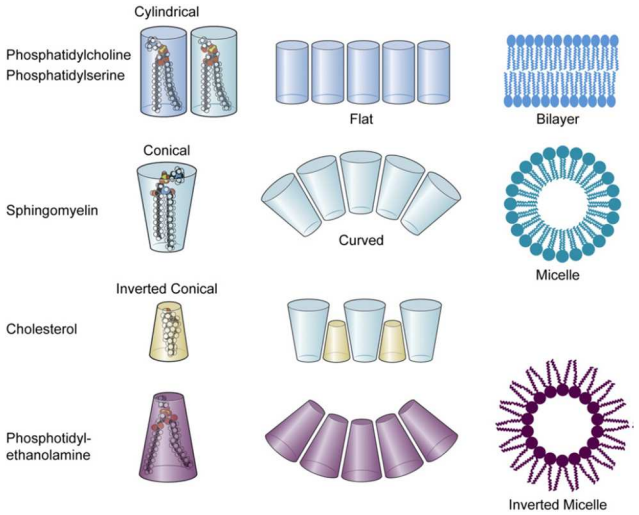

Figure 9. Schematic diagram depicting molecular shape-volumes occupied by various membrane lipid types. Image taken from[88].

1.5.1(b) Membrane rigidity and thickness

The length and saturation of lipid fatty acid (FA) chains determines both the thickness and rigidity of a liposome membrane. FA chain length within biological membranes typically varies between C12 and C30 – the number of carbon atoms – where a membrane made up of C30 lipids is approximately twice as thick one made up of C12 lipids. A mismatch of different FA chain lengths within a single membrane can lead to phase separation – where FAs of one particular length preferentially assemble together with one another. This can create specific lipid domains within a single continuous lipid membrane.[90]

FA chains can also be saturated (no double bonds) or unsaturated (1 or more double bond). In general, saturated FAs pack closely together to form rigid lipid membranes. In contrast, unsaturated FAs – with a bend in their FA chains as a result of the double bond – loosely pack to form fluid membranes.[91] These differences are characterized by variations in melting temperatures (T_m), defined as the temperature at which a lipid membrane transitions between the 'rigid' gel state and the 'fluid' liquid crystalline state.[92] Whereas the T_m of DSPC – a saturated C18:0 PC lipid – is 55^{o}C, its unsaturated orthologue, DOPC has a T_m of -17^{o}C. The 'fluidity' of liposome membranes is an important consideration in designing liposomal drug carriers as small molecules will more readily leak across fluid membranes than more closely packed ones.

1.5.1(c) Addition of cholesterol

Cholesterol – an endogenous and ubiquitous sterol within the body – rigidifies 'fluid' lipid membranes and makes more fluid 'rigid' lipid membranes.[93] As such it is helpful to think of cholesterol as a molecular 'cork' – plugging the 'gaps' to stabilize fluid lipid membranes and acting as a 'wedge' to destabilize rigid membranes. Cholesterol is often used to fine tune drug retention and release profiles of liposome-drug vectors.[94]

1.5.1(d) Liposome surface functionalization

Surface modification of liposome surfaces, for instance functionalization with active targeting moieties including antibodies and peptides,[88] can be achieved either

through incorporation of pre-synthesized lipidated reagents during formulation or through post-functionalization of pre-formed liposomes. Various conjugation strategies (*e.g.* click chemistry) have been used to successfully functionalize pre-formed liposomes.[95] As mentioned previously, PEGylation of liposome surfaces is known to reduce serum protein adsorption to the liposome surface, prolong circulation lifetimes in the body and maximize passive targeting of solid tumors via the EPR effect.[96] In the case of PEG_{2000}, approximately 5 mol% lipid-PEG reagents are required to sterically shield the entire liposome surface. Above 9 mol% PEG_{2000} and the brush-like arrangement of PEG on the liposome surface is thought to destabilize the lipid bilayer.[24a]

1.5.1.1 DePEGylation of liposome surfaces to reveal new functionalities

Through dePEGylation it is possible to reveal underlying functionality to promote drug delivery to target cells. Shielding functionality *en route* to the target tumor also reduces the risk of off-target interactions with non-target cells. In this vein, several strategies have been investigated and three of them are highlighted in Figure 10.[60f, 97]

In the first example, a liposome surface was functionalized with two different PEG-lipid conjugates whose PEG chains varied in length (PEG_{2000} and PEG_{1000}) (Figure 10a).[68c] To the longer PEG_{2000} arm a monoclonal antibody, (mAb) 2C5, previously shown to specifically target a range of human cancer cell lines, was conjugated.[98] To the shorter PEG_{1000} arm the cell-penetrating TAT peptide was attached.[99] In the absence of MMP enzymes, the longer PEG_{2000} effectively shielded the underlying function of the TAT peptide, preventing non-specific cellular interactions, while the 2C5 promoted specific binding to cancer cells. In the presence of MMP enzymes – *i.e.* within the tumor microenvironment – PEG_{2000} was efficiently cleaved, revealing underlying TAT functionality which enhanced the intracellular uptake of the liposome-drug carrier two-fold as compared to liposomes lacking the TAT peptide.

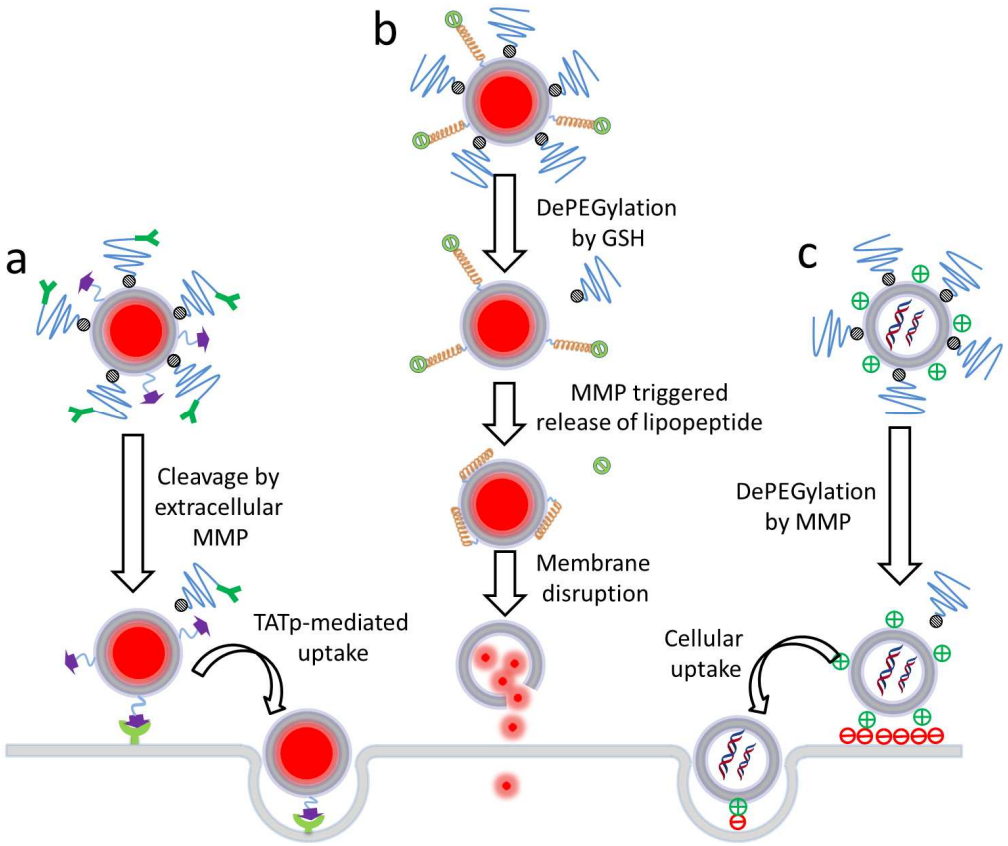

Figure 10. Illustration of PEGylation strategies on different types of liposomes, (A) PEGylated targeted liposomes, (B) PEGylated liposomes with membrane destabilizing peptides, (C) PEGylated cationic liposomes.

A similar dual responsive strategy was employed to promote extracellular drug release within the tumor microenvironment (Figure 10b). In this case, dePEGylation of longer PEG_{2000} arms was triggered by an increase of extracellular GSH within the tumor microenvironment.[100] This in turn revealed underlying functionality, which when catalyzed by MMP, released a membrane lytic peptide. In this way, quantitative drug (*i.e.* gemcitabine) release in both 2D and 3D "tumor-like" spheroid cultures as well as suppressed tumor growth in mice following intravenous administration of gemcitabine-encapsulated liposomes was demonstrated. As drug release required exposure to both reductant and protease enzymes, this approach greatly minimized the risk of premature activation and drug release.

DePEGylation has also been successfully used to reveal underlying liposome surface charge (Figure 10c). Cationic liposomes are often employed as a gene delivery system owing to their potential to efficiently condense and protect polyanionic DNA and RNA.[101] However, cationic nanoparticles are rapidly cleared from circulation due to both non-specific interactions with anionic cell surfaces and extensive adsorption of serum components (opsonisation) and clearance *via* the MPS.[101] Both extracellular enzymatic [29] and intracellular[52] acid catalyzed dePEGylation strategies have been shown to increase the transfection/transduction efficiencies of cationic gene vectors.

1.5.1.2 DePEGylation of liposome surfaces to destabilize liposome membranes

DePEGylation of liposomes has also been used to destabilize the integrity of the liposome membrane itself to trigger drug release. In these cases, dePEGylation results in a change of lipid geometry (*i.e.* loss of large hydrophilic PEG headgroup) generating a lipid composition which no longer packs to form a stable lipid bilayer. By utilizing a cholesteryl hemisuccinate (CHEMS)-PEG conjugate, Dong *et al.* were able to successfully demonstrate dePEGylation – triggered by enzymatic cleavage of the CHEMS-PEG ester linkage – following endocytotic uptake. Subsequent protonation of the newly revealed CHEMS carboxylate groups, within the acidic endosome, resulted in rapid liposome rupture and content release.[102] This approach did however rely on the cellular uptake of PEGylated liposomes, which as mentioned previously, is extremely slow.[103]

Another popular strategy has been to take advantage of the 'fusogenic' lipid, DOPE, which preferentially adopts a non-bilayer, hexagonal phase (H_{II}) in aqueous solution.[104] Cone-shaped DOPE can be incorporated at high concentrations within stable lipid bilayers consisting of cylinder and/or cone shaped lipids. If DOPE-rich bilayers are stabilized using a stimuli-responsive lipid-PEG conjugate, dePEGylation results in rapid membrane destabilization and concomitant content release (Figure 11).[47a]

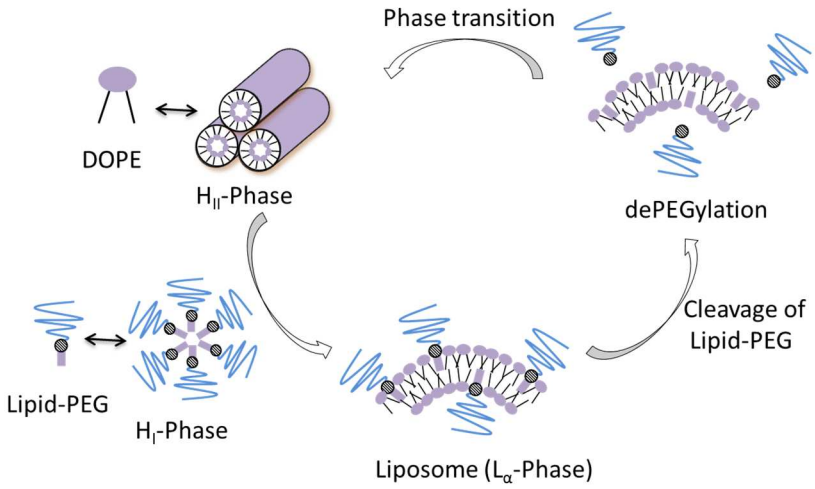

Figure 11. Destabilization of liposomes formed by DOPE and cleavable PEG–lipid upon dePEGylation. Image taken from[39a].

Zalipsky *et al.* reported the first example of a DOPE-rich liposome membrane stabilized using cone-shaped and redox-sensitive lipid-PEG_{2000} (mPEG-SS-DSPE) conjugates.[59] Incorporation of just 3 mol% lipid-PEG conjugate (*i.e.* 97 mol% DOPE) resulted in the formulation of stable liposomes, however in the presence of DTT – a thiolytic agent – loss of PEG led to rapid liposome destabilization and drug release. Inspired by this concept, numerous efforts have been made to design stimuli-responsive PEG-lipids to stabilize DOPE-rich liposomes. These have included dithiobenzyl (DTB) urethane,[61] diortho ester[45a] and vinylether[47b] lipid-PEG linkages.

1.5.2 Micelles

Micelles are formed through the self-assembly of cone-shaped amphiphiles in aqueous solution and are characterized by an inner hydrophobic core. Hydrophobic cargos/drugs can be efficiently packed within the micelle core and protected from the outside environment. Micelles have been widely investigated as potential DDS against a variety of human diseases including leukemia[105], hepatitis[106], breast cancer[107] and ovarian cancer.[108] An important consideration when using micelles is that the concentration of amphiphiles must be above the critical micelle concentration (CMC). Below this concentration, micelles disassemble in solution and as a result the drug/cargo is exposed.

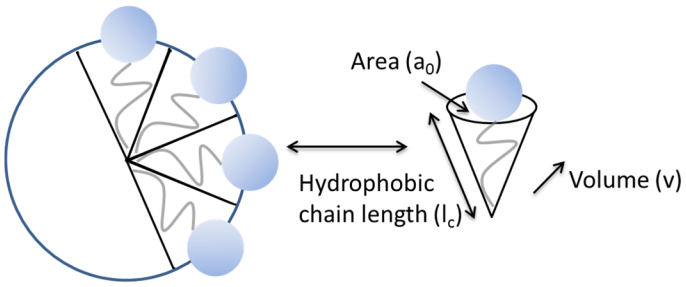

Name	Structure	Charge
Triton X-100	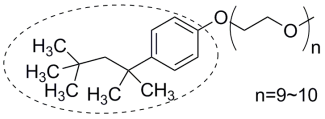	Non-ionic
Tween 20/40/60/80	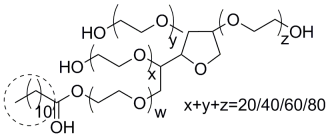	
Dodecyl sulfate	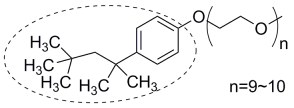	Anionic

Figure 12. The required geometry of molecules for micelle formation (top) and the structure of some common micelle-forming detergents (bottom); the dash line circled part is hydrophobic component.

To preferentially form micelles over other self-assembled structures, the surface area (a_o) of the hydrophilic head group must be sufficiently large, while the volume (v) of hydrophobic portion must be sufficiently small. Micelles are only formed when the geometric constraint, critical packing parameter ($P = v/a_o l_c$), of the molecules is < 1/3. (Figure 12).[109] Detergents like sodium dodecyl sulfate (SDS) are classic examples of lipid amphiphiles which preferentially form micelles in aqueous solutions.

PEGylated amphiphiles have a natural propensity to form micelles given the large surface area of the hydrophilic PEG headgroup. Upon dePEGylation however, cone-shaped molecular geometries are lost resulting in micelle destabilization. This leads to efficient drug release from the hydrophobic micelle core. Depending on the

hydrophobic component, micelle DDS can divided into lipid micelles, polymeric micelles, pro-drug micelles and hybrid micelles.

1.5.2.1 Lipid micelles

The most common lipid anchors used to form lipid-PEG amphiphiles have been DSPE[110], cholesterol[111] and fatty acids.[57d] Depending on the hydrophobicity of lipids, the molecular weight of the PEG block ranging from 750 to 5000 Da with the resultant micelle size ranging from tens to hundreds of nanometers have been used. To achieve stimuli responsive drug release, cleavable linkers are often incorporated between the PEG chain and lipid.[112] After accumulation at the site of a tumor, the dePEGylated micelles are internalized into endosomes/lysosomes, resulting in release of the drugs intracellularly.

1.5.2.2 Polymeric micelles

To obtain polymer-PEG micelles, hydrophobic and biocompatible/biodegradable polymers are required to form a stable hydrophobic micellar core. The most common synthetic polymers used in polymeric micelle designs are shown in Scheme 2.[57a] Stimuli responsive PEGylated polymeric micelles have been developed to be sensitive to both endogenous (*e.g.* redox[57a], pH[38, 79e]) and exogenous (*e.g.* light[38]) triggers.

Polypeptides, composed of natural and/or non-natural amino acids have also been widely used to from the hydrophobic core of PEGylated, polymeric micelle DDS. In one example, a redox-sensitive co-polymer composed of PEG and poly-L-leucine (PEG-SS-pLeu) was used to control the release of doxorubicin (DOX) under reducing conditions.[56b] The fully biocompatible system demonstrated no toxicity to cancer cells *in vitro* prior to dePEGylation but rapid and quantitative drug release in the reductive environment of endosomes.

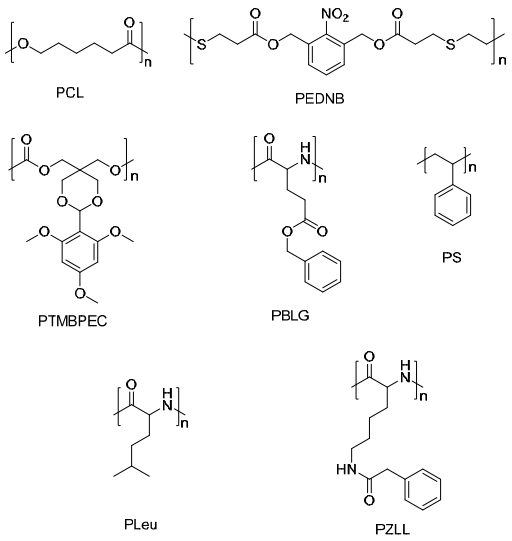

Scheme 2. Overview of polymer blocks conjugated to PEG used polymeric micelles.

1.5.2.3 Polyion complex (PIC) micelles

As a sub-group of polymeric micelles, PIC micelles have been investigated as potential non-viral gene vectors. These copolymer systems comprise a hydrophilic/ionic polymer conjugated to PEG, which upon complexation with oppositely charged cargos (*e.g.* DNA, RNA or protein) form micellar structures with a charge neutralized hydrophobic core (Figure 13a).[113] Depending on the associated charge of the complexed cargo, the hydrophilic/ionic polymer can be both polyanionic or polycationic. Common charged polymers used in PIC systems include poly (L-lysine) (PLL),[43a, 56l] poly (L-aspartate)(pAsp),[114] polyethylenimine (PEI)[60g, 68d] and poly(2-(dimethyl-amino)ethylmethacrylate) (PDMAEMA).[46a]

To extend the function of PIC micelles to the delivery of both hydrophilic and charged cargos as well as small molecule hydrophobic drugs, Torchilin and coworkers incorporated an additional hydrophobic DOPE core to a PEI-PEG polymer construct. In this way, the authors were able to efficiently encapsulate hydrophobic paclitaxel within the DOPE core and simultaneously condense siRNA as a complex with PEI to form a dual therapy (Figure 13b).[68d]

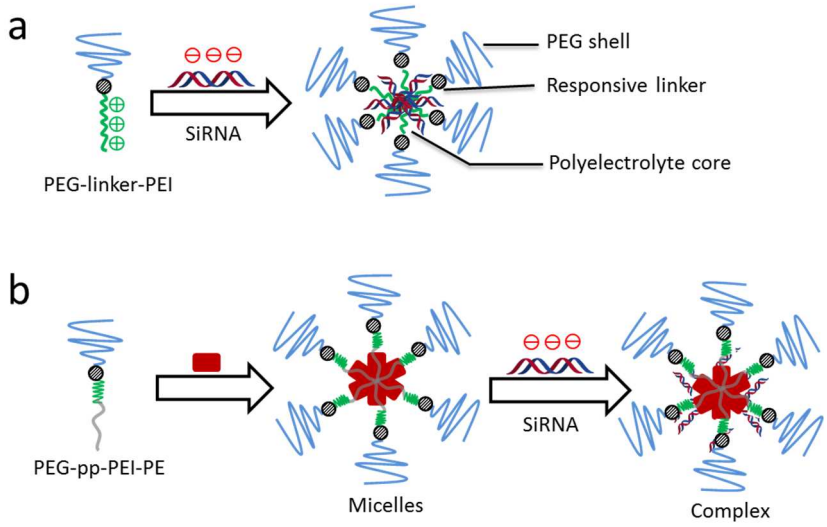

Figure 13. (a) Schematic illustration of PIC micelles formed by PEGylated cationic polymers with anionic biotherapeutics (*e.g.* siRNA). (b) Illustration of PIC micelles as carriers to co-deliver hydrophobic drugs.

1.5.2.4 Prodrug micelles

The principle limitations of polymeric and lipid micelle DDS are poor drug loading efficiencies and premature drug leakage from the micelle core. To address these issues, efforts have been made to develop prodrug micelle DDS in which the therapeutic drugs themselves are used to form the hydrophobic core of the micelle (Figure 14a).[115] The principle advantages of these systems are higher drug encapsulation efficiencies (w/w) and, as drugs are now covalently linked to the PEG corona, no premature drug leakage. A key disadvantage of these systems is sub-optimal packing of the hydrophobic micelle, resulting in decreased micelles stability.

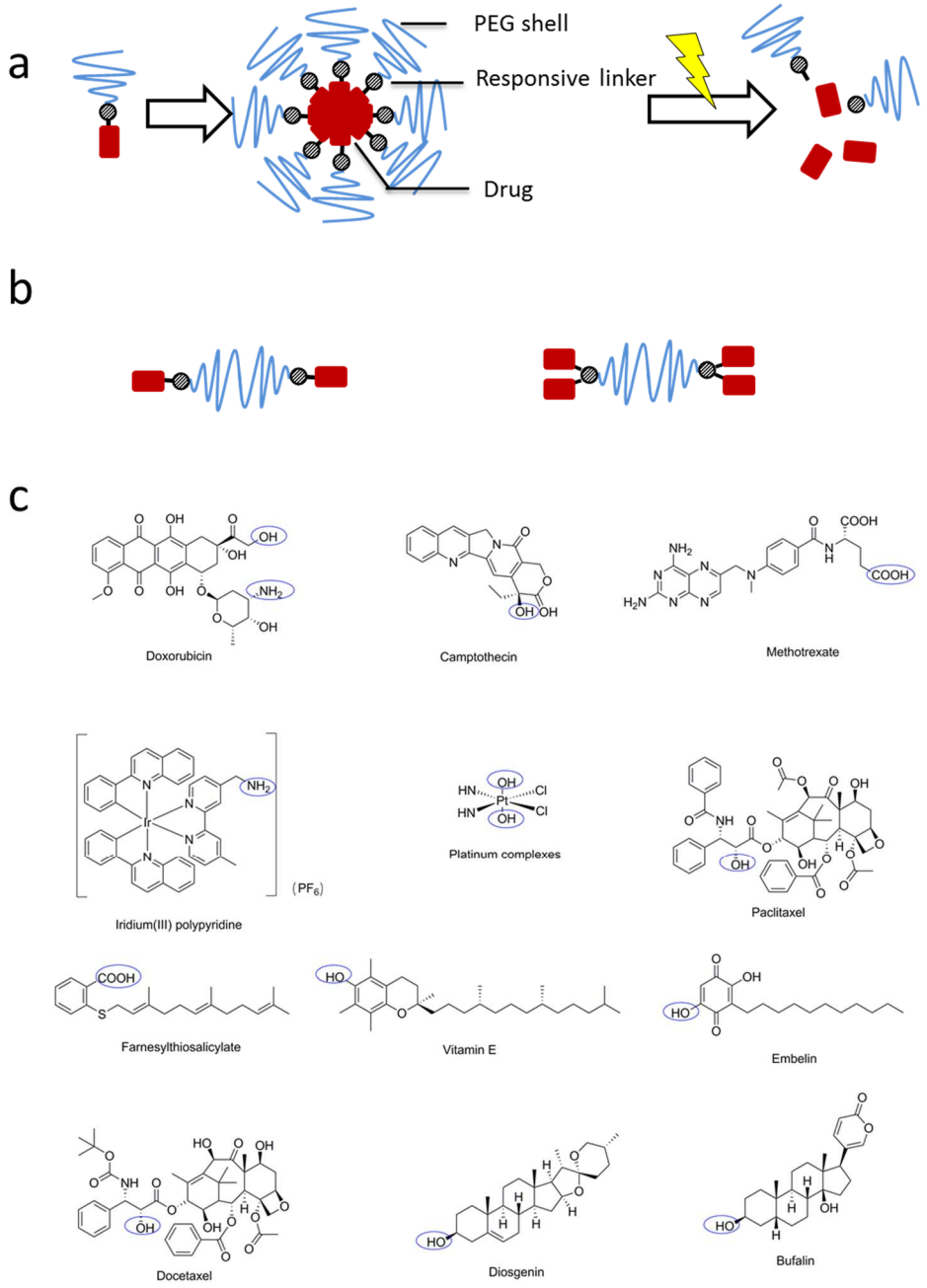

Figure 14. (a) Schematic illustration of micelles formed by PEGylated prodrugs; (b) two tailed prodrugs (c) The structure of anticancer drugs used in stimuli-sensitive PEGylated prodrugs (reactive groups in circles).

A variety of anticancer drugs have been used to construct PEGylated prodrug micelles. These include doxorubicin,[52a, 116] camptothecin,[117] methotrexate,[118] metallic antitumor agents,[86] bufalin,[119] vitamin E,[60h, 120] diosgenin,[121] paclitaxel,[122] embelin,[123] docetaxel[124] and farnesylthiosalicylic acid (FTS) (Figure 14c).[125]

To overcome the principle limitation of these systems – namely, low micelle stability due to a high CMC, efforts have been made to stabilize the hydrophobic core using higher drug/PEG ratio (Figure 14b). Wang *et al* investigated the correlation between DOX loading efficiency and PEG chain length (PEG_{2000}, PEG_{4000} and PEG_{6000}), onto which two DOX molecules were connected to each individual PEG chain through an acid-sensitive linkage.[126] They achieved up to 37% (w/w) DOX encapsulation (using PEG_{2000}), significantly higher than conventional drug loading method using polymeric micelles, and with greater micelle stability. In another report, Dong *et al* used a branched system to couple up to 8 methotrexate molecules to a single PEG polymer. This resulted in drug-rich pro-drug micelles (26% w/w) with improved *in vivo* stability.[56m]

1.5.2.6 Hybrid micelles

In many cases, micelles formed from the self-assembly of a single amphiphile building block do not fulfill the optimal requirements of an efficient micellar DDS. For instance, DOX-PEG prodrug micelles typically demonstrate high CMCs (*i.e.* low stability) owing to suboptimal packing of doxorubicin within the hydrophobic core of the micelle. Co-formulation and self-assembly of additional amphiphilic components, to form hybrid micelles, is a common strategy to improve micelle performance of a micellar DDS but also a simple way of adding additional functionality to an existing design.[127]

An elegant example of a multifunctional, hybrid micelle DDS combined a PEG_{2000}-paclitaxel conjugate, containing an MMP sensitive linkage (PEG_{2000}-MMP-PTX), together with cell penetrating peptide-PEG_{1000}-phosphoethanolamine (TATp-PEG_{1000}-DOPE) and PEG_{1000}-phosphoethanolamine (PEG_{1000}-DOPE) lipid amphiphiles in the ratio of 5:4:1 (mol/mol/mol).[66] Compared to micelles formed from PEG_{2000}-paclitaxel alone, these micelles were an order of magnitude more stable (3.9 μM vs 32 μM). In this system, the longer PEG_{2000} effectively shielded the

underlying TAT peptide function and extended circulation lifetimes *in vivo* following systemic administration. Once accumulated within the tumor microenvironment, MMP-mediated enzymatic cleavage of the PEG_{2000} corona revealed the underlying cell penetrating TAT-peptide, driving the efficient internalisation and intracellular drug delivery. Importantly, upon the loss of PEG_{2000}, micelles remained intact, stabilized by the remaining lipid-PEG_{1000}-TAT construct and containing paclitaxel within the hydrophobic core. This served to minimize extracellular release of paclitaxel within the tumor microenvironment. Adding further flexibility to the design of this system, Zhu *et al.* were able to successfully entrap free paclitaxel within the hydrophobic core of a PEG_{2000}-MMP-DOPE/ TATp-PEG_{1000}-DOPE hybrid micelle (Figure 15).[128] With no additional chemical modification to existing hydrophobic drugs required in this case, this system demonstrates the broad potential of such a hybrid micelle system in delivering diverse therapeutic cargos.

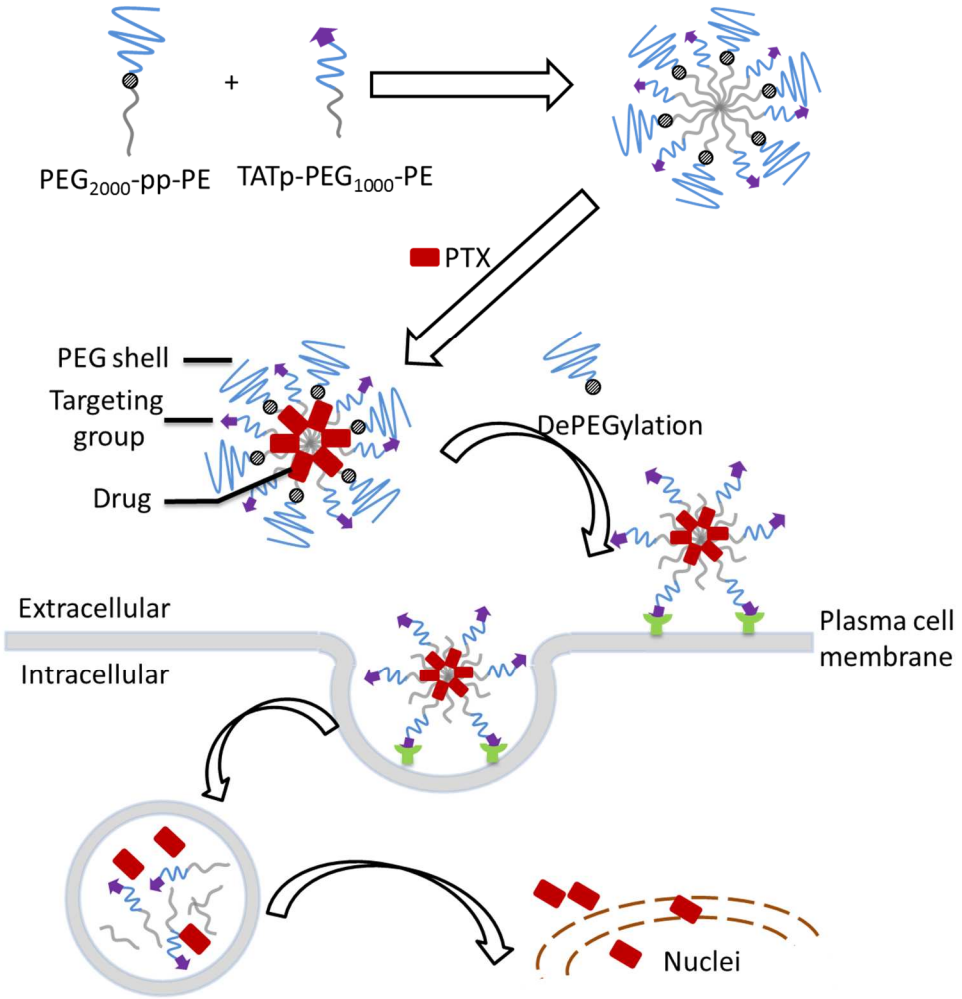

Figure 15. Illustration of hybrid micelles made of PEG2000-Pp-PE and TATp-PEG1000-PE to deliver free drugs.

1.5.3 Polymersomes

Polymersomes are artificial vesicles comprised of a polymer membrane surrounding an inner aqueous core.[129] Analogous to liposomes, it is possible to load hydrophilic drugs/cargos within the inner aqueous core and hydrophobic drugs within the polymersome membrane interior.[130] Common polymersome DDS are self-assembled nanostructures composed of linear diblock copolymer amphiphiles (hydrophilic-hydrophobic) or tri-block polymer bola-amphiphiles (hydrophilic-hydrophobic-hydrophilic). Typically, polymersomes are more stable than liposomes in aqueous solution, as reflected in their lower critical aggregation

concentrations (CAC).[131] Although many polymers (*e.g.* polyesters) are hydrolytically sensitive and degrade over time within the body, the rate of hydrolysis and polymersome destabilization, even under acid-catalyzed conditions (*e.g.* within endosomes), is generally too slow to result in the release of therapeutically relevant drug doses.

DePEGylation of polymersomes has been used as an effective method to rapidly destabilize polymersomes and promote drug release. In these systems, PEG is used as the hydrophilic block of a di- or tri-block polymer and is therefore an integral to polymersome self-assembly. Release of PEG (*i.e.* the hydrophilic block) leads to polymersome destabilization and concomitant drug release occurs. In one of the first examples of polymersome dePEGylation, Hubbell *et al*. where able to demonstrated efficient endosomal drug release from polymersomes composed of redox-sensitive PEG-S-S-poly(propylene sulfide) di-block copolymers.[132] In this case, polymersome cellular uptake, disruption and quantitative drug release occurred within 10 minutes of incubation with cells *in vitro*. Since then, many reductive PEG copolymers have been designed and applied as building blocks to construct redox-sensitive polymersomes.[55b, 56f, 57c, 133] Moreover, photo-degradable polymersomes could also be constructed by co-polymers with photo-cleavable moiety, such as PEG-*o*-NB-PCL.[80] In this kind of polymersomes, under a short UV exposure, content release was accompanied with partially-cleaved PEG and the rearrangement of PCL segments. However, the remaining PEG-PCL still stabilizes the vesicular structure. Only after full cleavage of PEG-PCL, collapse of polymersomes was observed.

1.6 Overview and goals of this thesis

From this review of current technologies, it is clear stimuli-responsive dePEGylation of nanoparticle-based DDS is an effective strategy to potentially enhance therapeutic efficacy. However, no such systems have yet made it to market. For this to happen, a clear cost-to-benefit advantage, over, for example, administering the free drug alone, must be demonstrated. This will only be realized if DDS systems are either simplified (to bring down development and manufacturing costs) and/or efficacy is improved.

The work in this thesis focuses on overcoming various technological inefficiencies associated with current stimuli-responsive nanoparticles. These include: enabling drug delivery directly to the cell cytosol (**chapter 2)**, optimizing physicochemical properties and drug retention/release profiles of pro-drug micelles (**chapter 3 and 4**) and exploiting the differing *in vivo* fates of nanoparticles with opposing surface charges (**chapter 5**). In all cases, activation is triggered by light, affording precise spatiotemporal control over where and when dePEGylation/activation occurs.

In **chapter 2**, spatiotemporal control of membrane fusion system is reported through photolabile PEGylation of fusogenic liposomes. In this system, fusion relies on the recognition and binding of complementary peptides displayed on opposing liposome surfaces. Peptide recognition can be efficiently inhibited through liposome surface PEGylation. Light triggered fusion was demonstrated in both liposome-liposome systems and between liposomes and cells. This system paves the way towards controlled drug delivery direct to the cytosol of cells thereby avoiding endocytosis.

In **chapters 3 and 4**, two PEGylated prodrugs, PEG_{2000}-*o*-nitrobenzyl-doxorubicin (**chapter 3**) and PEG_{2000}-*o*-nitrobenzyl-nervonic acid (**chapter 4**) are described. Both conjugates self-assembled into micelles in aqueous solution with the PEG layer as the outer corona. In **chapter 3**, the release behavior of conjugated doxorubicin (DOX) from micelles was investigated and precise spatiotemporal control of drug delivery to cells demonstrated.

In **chapter 4,** a very long chain fatty acid (nervonic acid, NA) was conjugated to PEG via a photo-cleavable linker. Forming close packed micelles, this enabled the efficient incorporation of highly insoluble NA into target cellular membranes. Subsequent photolysis of PEG released free NA, which was subsequently processed by the cells to form very long chain phospholipids. This is expected to result in the thickening of the plasma cell membrane and provides an indirect method to modulate membrane protein activity.

In **chapter 5**, novel cationic lipids were photocaged to form neutral, caged cationic lipids. These could be formulated into liposomes which were shown to be freely circulating following intravenous injection *in vivo*. Following UV irradiation resulting in

photolysis of *o*-Nb, the liposome surface charge rapidly switched from neutral to cationic leading to the non-specific cellular adsorption, uptake and intracellular drug delivery of liposome encapsulated cargos. Switching of surface charge was demonstrated *in situ* and *in vivo* and importantly did not lead to content leakage from the liposome drug carrier.

Finally, in **chapter 6**, the main results and conclusions of this thesis are summarized and the advantages and future perspectives of using photo-cleavable DDS are described.

1.7 References

[1] R. M. McQuade, V. Stojanovska, R. Abalo, J. C. Bornstein, K. Nurgali, *Front Pharmacol* **2016**, *7*.

[2] S. W. Y. Atiar M Rahman, Michael S Ewer, *Int J Nanomedicine* **2007**, *2*, 567–583.

[3] Y. H. Bae, K. Park, *J Control Release* **2011**, *153*, 198-205.

[4] (a) A. Beck, L. Goetsch, C. Dumontet, N. Corvaia, *Nat Rev Drug Discov* **2017**, *16*, 315-337; (b) H. I. Chang, M. K. Yeh, *Int J Nanomedicine* **2012**, *7*, 49-60.

[5] S. C. Alley, N. M. Okeley, P. D. Senter, *Curr Opin Chem Biol* **2010**, *14*, 529-537.

[6] H. L. Perez, P. M. Cardarelli, S. Deshpande, S. Gangwar, G. M. Schroeder, G. D. Vite, R. M. Borzilleri, *Drug Discov Today* **2014**, *19*, 869-881.

[7] R. Haag, *Angew Chem Int Edit* **2004**, *43*, 278-282.

[8] E. Blanco, H. Shen, M. Ferrari, *Nat Biotechnol* **2015**, *33*, 941-951.

[9] H. Maeda, H. Nakamura, J. Fang, *Adv Drug Deliv Rev* **2013**, *65*, 71-79.

[10] L. M. Russell, M. Hultz, P. C. Searson, *J Control Release* **2018**, *269*, 171-176.

[11] H. Maeda, *Journal of Controlled Release* **2012**, *164*, 138-144.

[12] S. Wilhelm, A. J. Tavares, Q. Dai, S. Ohta, J. Audet, H. F. Dvorak, W. C. W. Chan, *Nat Rev Mater* **2016**, *1*.

[13] T. Lammers, F. Kiessling, W. E. Hennink, G. Storm, *J Control Release* **2012**, *161*, 175-187.

[14] M. W. Dewhirst, T. W. Secomb, *Nat Rev Cancer* **2017**, *17*, 738-750.

[15] J. I. Hare, T. Lammers, M. B. Ashford, S. Puri, G. Storm, S. T. Barry, *Adv Drug Deliver Rev* **2017**, *108*, 25-38.

[16] R. J. Y. H. T. Lian, *J Pharm Sci* **2001**, *90*, 667-680.

[17] A. Akbarzadeh, R. Rezaei-Sadabady, S. Davaran, S. W. Joo, N. Zarghami, Y. Hanifehpour, M. Samiei, M. Kouhi, K. Nejati-Koshki, *Nanoscale Res Let* **2013**, *8*.567-578

[18] M. A. Clond, B. S. Lee, J. J. Yu, M. B. Singer, T. Amano, A. W. Lamb, D. Drazin, B. Kateb, E. J. Ley, J. S. Yu, *Plos One* **2013**, *8*.1026-1030

[19] M. Longmire, P. L. Choyke, H. Kobayashi, *Nanomedicine (Lond)* **2008**, *3*, 703-717.

[20] Y. N. Zhang, W. Poon, A. J. Tavares, I. D. McGilvray, W. C. W. Chan, *J Control Release* **2016**, *240*, 332-348.

[21] P. Aggarwal, J. B. Hall, C. B. McLeland, M. A. Dobrovolskaia, S. E. McNeil, *Adv Drug Deliv Rev* **2009**, *61*, 428-437.

[22] A. Kolate, D. Baradia, S. Patil, I. Vhora, G. Kore, A. Misra, *J Control Release* **2014**, *192*, 67-81.

[23] W. Li, P. Zhan, E. De Clercq, H. Lou, X. Liu, *Prog Polym Sci* **2013**, *38*, 421-444.

[24] (a)G. Pasut, F. M. Veronese, *J Control Release* **2012**, *161*, 461-472; (b)P. L. Turecek, M. J.Bossard, F. Schoetens, I. A. Ivens, *J Pharm Sci* **2016**, *105*, 460-475.

[25] Y. Maitani, *J Drug Deliv Sci Technol* **2011**, *21*, 27-34.

[26] R. P. Garay, R. El-Gewely, J. K. Armstrong, G. Garratty, P. Richette, *Expert Opin Drug Del* **2012**, *9*, 1319-1323.

[27] H. Schellekens, W. E. Hennink, V. Brinks, *Pharm Res-Dordr* **2013**, *30*, 1729-1734.

[28] H. Hatakeyama, H. Akita, H. Harashima, *Adv Drug Deliv Rev* **2011**, *63*, 152-160.

[29] H. Y. Xue, P. B. Guo, W. C. Wen, H. L. Wong, *Cur Pharm Des* **2015**, *21*, 3140-3147.

[30] C. H. John W. Holland, Pieter R. Cullis, and Thomas D. Madden, *Biochemistry-Us* **1996**, *35*, 2618-2624.

[31] J. R. S. a. M. J. Zuckermann, *Biochemistry-Us* **1993**, *32*, 3153-3161.

[32] W. M. Li, L. Xue, L. D. Mayer, M. B. Bally, *Bba-Biomembranes* **2001**, *1513*, 193-206.

[33] M. B. B. Gitanjali Adlakha-Hutcheon, Clifford R. Shew and Thomas D. Madden, *Nat Biotech* **1999**, *17*, 775-779.

[34] S. Khondee, C. M. Olsen, Y. Zeng, C. R. Middaugh, C. Berkland, *Biomacromolecules* **2011**, *12*, 3880-3894.

[35] B. Romberg, W. E. Hennink, G. Storm, *Pharm Res* **2008**, *25*, 55-71.

[36] S. Mura, J. Nicolas, P. Couvreur, *Nat Mater* **2013**, *12*, 991-1003.

[37] (a) S. S. Motoi Oishi, Yukio Nagasaki and Kazunori Kataoka, *Biomacromolecules* **2003**, *4*, 1426-1432; (b) M. Oishi, F. Nagatsugi, S. Sasaki, Y. Nagasaki, K. Kataoka, *Chembiochem* **2005**, *6*, 718-725; (c) Y. N. Motoi Oishi, Keiji Itaka, Nobuhiro Nishiyama and Kazunori Kataoka, *J. Am. Chem. Soc.* **2005**, *127*, 1624-1625; (d) Z. Y. Lin Zhu, Kun Cheng, Duane D. Miller, and Ram I. Mahato, *Bioconjugate Chem* **2008**, *19*, 290–298.

[38] Q. Jin, T. Cai, H. Han, H. Wang, Y. Wang, J. Ji, *Macromol Rapid Commun* **2014**, *35*, 1372-1378.

[39] S. W. K. Ji Hoon Jeong, and Tae Gwan Park, *Bioconjugate Chem.* **2003**, *14*, 473−479.

[40] N. Nischan, A. Chakrabarti, R. A. Serwa, P. H. Bovee-Geurts, R. Brock, C. P. Hackenberger, *Angew Chem Int Ed Engl* **2013**, *52*, 11920-11924.

[41] C. L. Chan, R. N. Majzoub, R. S. Shirazi, K. K. Ewert, Y. J. Chen, K. S. Liang, C. R. Safinya, *Biomaterials* **2012**, *33*, 4928-4935.

[42] F. Li, J. He, M. Zhang, K. C. Tam, P. Ni, *RSC Adv.* **2015**, *5*, 54658-54666.

[43] (a)G. F. Walker, C. Fella, J. Pelisek, J. Fahrmeir, S. Boeckle, M. Ogris, E. Wagner, *Mol Ther* **2005**, *11*, 418-425; (b)F. Li, J. He, M. Zhang, P. Ni, *Polym. Chem.* **2015**, *6*, 5009-5014.

[44] (a)J. A. M. Joon Sig Choi, and Francis C. Szoka, Jr., *Bioconjugate Chem* **2003**, *14*, 420−429; (b)J. A. M. Xin Guo, y and Francis C. Szoka, Jr.z, *Biophys J* **2003**, *84*, 1784–1795.

[45] (a)X. G. a. F. C. S. Jr., *Bioconjugate Chem* **2001**, *12*, 291−300; (b)C. Masson, M. Garinot, N. Mignet, B. Wetzer, P. Mailhe, D. Scherman, M. Bessodes, *J Control Release* **2004**, *99*, 423-434.

[46] (a) F. D. Song Lin, Yang Wang, Shouping Ji, Zichen Li, *Biomacromolecules* **2008**, *9*, 109–115; (b) R. Ji, J. Cheng, T. Yang, C. C. Song, L. Li, F. S. Du, Z. C. Li, *Biomacromolecules* **2014**, *15*, 3531-3539.

[47] (a) J. Shin, *J Control Release* **2003**, *91*, 187-200; (b) H. D. I. Jeremy A. Boomer, Zhi-Yi Zhang, Nill Bergstrand, Katarina Edwards, Jong-Mok Kim and David H. Thompson, *Langmuir* **2003**, *19*, 6408-6415; (c) W. G. Zhenghong Xu, Lingli Chen, Yu Gao, Zhiwen Zhang, and Yaping Li, *Biomacromolecules* **2008**, *9*, 3119–3126; (d) J. Shin, P. Shum, J. Grey, S. Fujiwara, G. S. Malhotra, A. Gonzalez-Bonet, S. H. Hyun, E. Moase, T. M. Allen, D. H. Thompson, *Mol Pharm* **2012**, *9*, 3266-3276; (e) H. K. Kim, J. Van den Bossche, S. H. Hyun, D. H. Thompson, *Bioconjug Chem* **2012**, *23*, 2071-2077; (f) M. M. Q. Jeremy A. Boomer, H. Dorota Inerowicz, Robert H. Haynes, V. Srilakshmi Patri, Jong-Mok Kim, and David H. Thompson, *Bioconjugate Chem.* **2009**, *20*, 47–59.

[48] W.-P. C. Jingxia Gu, Xiaozhong Qu, Jiguang Liu, Sum-Yee Lo and Zhenzhong Yang, *Biomacromolecules* **2008**, *9*, 255–262.

[49] H. Rongbin, X. Lei, L. Ying, D. Xiangping, C. Xuan, L. Lanfang, Y. Cuiyun, C. Yanming, T. Guotao, *J Pharm Pharmacol* **2016**, *68*, 751-761.

[50] J. Li, L. Zhang, Y. Lin, H. Xiao, M. Zuo, D. Cheng, X. Shuai, *RSC Adv.* **2016**, *6*, 9160-9163.

[51] (a)J. Wang, C. Gong, Y. Wang, G. Wu, *Colloids Surf B Biointerfaces* **2014**, *118*, 218-225; (b)J. Wang, C. Gong, Y. Wang, G. Wu, *RSC Adv* **2014**, *4*, 15856.

[52] (a)D. Sun, J. Ding, C. Xiao, J. Chen, X. Zhuang, X. Chen, *ACS Appl Mater Interfaces* **2014**, *6*, 21202-21214; (b)D. Sun, J. Ding, C. Xiao, J. Chen, X. Zhuang, X. Chen, *Adv Healthc Mater* **2015**, *4*, 844-855.

[53] T. Sun, A. Morger, B. Castagner, J. C. Leroux, *Chem Commun (Camb)* **2015**, *51*, 5721-5724.

[54] Q. L. Li, S. H. Xu, H. Zhou, X. Wang, B. A. Dong, H. Gao, J. Tang, Y. W. Yang, *Acs Appl Mater Inter* **2015**, *7*, 28656-28664.

[55] (a) T. H. Motoi Oishi, Yoshitsugu Akiyama, Seiji Takae, Atsushi Harada, Yuichi Yamasaki, Fumi Nagatsugi, Shigeki Sasaki, Yukio Nagasaki and Kazunori Kataoka, *Biomacromolecules* **2005**, *6*, 2449-2454; (b) L. Jia, D. Cui, J. Bignon, A. Di Cicco, J. Wdzieczak-Bakala, J. Liu, M. H. Li, *Biomacromolecules* **2014**, *15*, 2206-2217; (c) H. Gong, Z. Xie, M. Liu, H. Sun, H. Zhu, H. Guo, *Colloid and Polym Sci* **2015**, *293*, 2121-2128; (d) Y. Wang, N. Han, Q. Zhao, L. Bai, J. Li, T. Jiang, S. Wang, *Eur J Pharm Sci* **2015**, *72*, 12-20; (e) H. Gong, Z. Xie, M. Liu, H. Zhu, H. Sun, *RSC Adv.* **2015**, *5*, 59576-59582.

[56] (a) X. Q. Li, H. Y. Wen, H. Q. Dong, W. M. Xue, G. M. Pauletti, X. J. Cai, W. J. Xia, D. Shi, Y. Y. Li, *Chem Commun (Camb)* **2011**, *47*, 8647-8649; (b) T.-B. Ren, W.-J. Xia, H.-Q. Dong, Y.-Y. Li, *Polymer* **2011**, *52*, 3580-3586; (c) Q. Guo, P. Luo, Y. Luo, F. Du, W. Lu, S. Liu, J. Huang, J. Yu, *Colloids Surf B Biointerfaces* **2012**, *100*, 138-145; (d) H. Wen, C. Dong, H. Dong, A. Shen, W. Xia, X. Cai, Y. Song, X. Li, Y. Li, D. Shi, *Small* **2012**, *8*, 760-769; (e) K. Wang, Y. Liu, W.-J. Yi, C. Li, Y.-Y. Li, R.-X. Zhuo, X.-Z. Zhang, *Soft Matter* **2013**, *9*, 692-699; (f) T. Ren, W. Wu, M. Jia, H. Dong, Y. Li, Z. Ou, *ACS Appl Mater Interfaces* **2013**, *5*, 10721-10730; (g) Y. Ping, Q. Hu, G. Tang, J. Li, *Biomaterials* **2013**, *34*, 6482-6494; (h) J. Yu, X. Li, Y. Luo, W. Lu, J. Huang, S. Liu, *Colloids Surf B Biointerfaces* **2013**, *107*, 213-219; (i) W. Chen, P. Zhong, F. Meng, R. Cheng, C. Deng, J. Feijen, Z. Zhong, *J Control Release* **2013**, *169*, 171-179; (j) J. Ding, J. Chen, D. Li, C. Xiao, J. Zhang, C. He, X. Zhuang, X. Chen, *J. Mater. Chem. B* **2013**, *1*, 69-81; (k) T. Thambi, G. Saravanakumar, J.-U. Chu, R. Heo, H. Ko, V. G. Deepagan, J.-H. Kim, J. H. Park, *Macromol Res* **2012**, *21*, 100-107; (l) H. Zhu, C. Dong, H. Dong, T. Ren, X. Wen, J. Su, Y. Li, *ACS Appl Mater Interfaces* **2014**, *6*, 10393-10407; mH. Dong, C. Dong, W. Xia, Y. Li, T. Ren, *Med. Chem. Commun.* **2014**, *5*, 147-152; (n) C. Cui, P. Yu, M. Wu, Y. Zhang, L. Liu, B. Wu, C. X. Wang, R. X. Zhuo, S. W. Huang, *Colloids Surf B Biointerfaces* **2015**, *129*, 137-145; (o) W. Hou, F. Xia, C. S. Alves, X. Qian, Y. Yang, D. Cui, *ACS Appl Mater Interfaces* **2016**, *8*, 1447-1457.

[57] (a) H. Sun, B. Guo, R. Cheng, F. Meng, H. Liu, Z. Zhong, *Biomaterials* **2009**, *30*, 6358-6366; (b) Y. Zhong, W. Yang, H. Sun, R. Cheng, F. Meng, C. Deng, Z. Zhong, *Biomacromolecules* **2013**, *14*, 3723-3730; (c) X. Wang, H. Sun, F. Meng, R. Cheng, C. Deng, Z. Zhong, *Biomacromolecules* **2013**, *14*, 2873-2882; (d) C. Cui, Y. N. Xue, M. Wu, Y. Zhang, P. Yu, L. Liu, R. X. Zhuo, S. W. Huang, *Biomaterials* **2013**, *34*, 3858-3869; (e) L. Jia, Z. Li, D. Zhang, Q. Zhang, J. Shen, H. Guo, X. Tian, G. Liu, D. Zheng, L. Qi, *Polym. Chem.* **2013**, *4*, 156-165; (f) Y. Cao, J. Zhao, Y. Zhang, J. Liu, J. Liu, A. Dong, L. Deng, *RSC Adv.* **2015**, *5*, 28060-28069.

[58] Y. Wang, Q. J. Luo, L. L. Gao, C. Gao, H. Du, G. Y. Zha, X. D. Li, Z. Q. Shen, W. P. Zhu, *Biomater Sci-Uk* **2014**, *2*, 1367-1376.

[59] K. H. Dmitri Kirpotin, Nasreen Mullah, Demetrios Papahadjopoulos, Samuel Zalipsky *FEBS Letters* **1996**, *388*, 115- 118.

[60] (a) S. H. Kim, J. H. Jeong, S. H. Lee, S. W. Kim, T. G. Park, *J Control Release* **2008**, *129*, 107-116; (b) K. M. McNeeley, E. Karathanasis, A. V. Annapragada, R. V. Bellamkonda, *Biomaterials* **2009**, *30*, 3986-3995; (c) W. Y. Rui Kuai, Yao Qin, Huali Chen, Jie Tang, Mingqing Yuan, Zhirong Zhang, and Qin He, *Mol Pharmaceutics* **2010**, *7*, 1816–1826; (d) Y. Cui, H. Dong, X. Cai, D. Wang, Y. Li, *ACS Appl Mater Interfaces* **2012**, *4*, 3177-3183; (e) L. Mei, L. Fu, K. Shi, Q. Zhang, Y. Liu, J. Tang, H. Gao, Z. Zhang, Q. He, *Int J Pharm* **2014**, *468*, 26-38; (f) J. Tang, H. Fu, Q. Kuang, L. Zhang, Q. Zhang, Y. Liu, R. Ran, H. Gao, Z. Zhang, Q. He, *J Drug Target* **2014**, *22*, 313-326; (g) J. M. Williford, Y. Ren, K. Huang, D. Pan, H. Q. Mao, *J Mater Chem B Mater Biol*

Med **2014**, *2*, 8106-8109; (h) X. Ai, J. Sun, L. Zhong, C. Wu, H. Niu, T. Xu, H. Lian, X. Han, G. Ren, W. Ding, J. Wang, X. Pu, Z. He, *Macromol Biosci* **2014**, *14*, 1415-1428.

[61] M. Q. Samuel Zalipsky, John A. Walker, Nasreen Mullah, Yolanda P. Quinn, and Shi Kun Huang, *Bioconjugate Chem* **1999**, *10*, 703-707.

[62] R. K. E. Charles C. Pak, Patrick L. Ahl, Andrew S. Janoį, Paul Meers, *Biochimica et Biophysica Acta* **1999**, *1419* 111-126.

[63] L. L. H. Benjamin E.Turk, Elizabeth T. Piro, and Lewis C. Cantley, *Nat biotechnol* **2001**, *19*, 661-667.

[64] P. Yingyuad, M. Mevel, C. Prata, S. Furegati, C. Kontogiorgis, M. Thanou, A. D. Miller, *Bioconjug Chem* **2013**, *24*, 343-362.

[65] C. Nazli, G. S. Demirer, Y. Yar, H. Y. Acar, S. Kizilel, *Colloids Surf B Biointerfaces* **2014**, *122*, 674-683.

[66] L. Zhu, T. Wang, F. Perche, A. Taigind, V. P. Torchilin, *Proc Natl Acad Sci U S A* **2013**, *110*, 17047-17052.

67] S. J. Lee, Y. I. Jeong, H. K. Park, D. H. Kang, J. S. Oh, S. G. Lee, H. C. Lee, *Int J Nanomedicine* **2015**, *10*, 5489-5503.

[68] (a) T. Terada, M. Iwai, S. Kawakami, F. Yamashita, M. Hashida, *J Control Release* **2006**, *111*, 333-342; (b) H. Hatakeyama, H. Akita, K. Kogure, M. Oishi, Y. Nagasaki, Y. Kihira, M. Ueno, H. Kobayashi, H. Kikuchi, H. Harashima, *Gene Ther* **2007**, *14*, 68-77; (c) P. K. Lin Zhu, and Vladimir P. Torchilin, *ACS Nano* **2012**, *6*, 3491**–**3498; (d) L. Zhu, F. Perche, T. Wang, V. P. Torchilin, *Biomaterials* **2014**, *35*, 4213-4222; (e) K. L. Veiman, K. Kunnapuu, T. Lehto, K. Kiisholts, K. Parn, U. Langel, K. Kurrikoff, *J Control Release* **2015**, *209*, 238-247; (f) Y. Tu, L. Zhu, *J Control Release* **2015**, *212*, 94-102; (g) Z. Dai, Q. Yao, L. Zhu, *ACS Appl Mater Interfaces* **2016**, *8*, 12661-12673.

[69] (a) J. Zhang, *Pharm Res* **2004**, *49*, 185-198; (b) Y. J. Zhong, L. H. Shao, Y. Li, *Int J Oncol* **2013**, *42*, 373-383.

[70] C. G. Bochet, *J Chem Soc Perk T 1* **2002**, 125-142.

[71] A. P. Castano, P. Mroz, M. R. Hamblin, *Nat Rev Cancer* **2006**, *6*, 535-545.

[72] C. M. Allen, W. M. Sharman, J. E. Van Lier, *J Porphyr Phthalocya* **2001**, *5*, 161-169.

[73] T. J. McMillan, E. Leatherman, A. Ridley, J. Shorrocks, S. E. Tobi, J. R. Whiteside, *J Pharm Pharmacol* **2008**, *60*, 969-976.

[74] S. H. Yun, S. J. J. Kwok, *Nat Biomed Eng* **2017**, *1*.

[75] L. Fournier, C. Gauron, L. Xu, I. Aujard, T. Le Saux, N. Gagey-Eilstein, S. Maurin, S. Dubruille, J. B. Baudin, D. Bensimon, M. Volovitch, S. Vriz, L. Jullien, *ACS Chem Biol* **2013**, *8*, 1528-1536.

[76] X. M. M. Weyel, M. A. H. Fichte, A. Heckel, *ACS Chem Biol* **2017**, *12*, 2183-2190.

[77] K. Peng, I. Tomatsu, B. van den Broek, C. Cui, A. V. Korobko, J. van Noort, A. H. Meijer, H. P. Spaink, A. Kros, *Soft Matter* **2011**, *7*, 4881.

[78] (a) Y. V. Il'ichev, M. A. Schworer, J. Wirz, *J Am Chem Soc* **2004**, *126*, 4581-4595; (b) I. Aujard, C. Benbrahim, M. Gouget, O. Ruel, J. B. Baudin, P. Neveu, L. Jullien, *Chem Eur J* **2006**, *12*, 6865-6879.

[79] (a) F. B. Peters, A. Brock, J. Wang, P. G. Schultz, *Chem Biol* **2009**, *16*, 148-152; (b) J.-M. Schumers, J.-F. Gohy, C.-A. Fustin, *Polym. Chem.* **2010**, *1*, 161-163; (c) J. M. Govan, A. L. McIver, A. Deiters, *Bioconjug Chem* **2011**, *22*, 2136-2142; (d) L. Li, A. Lv, X. X. Deng, F. S. Du, Z. C. Li, *Chem Commun (Camb)* **2013**, *49*, 8549-8551; (e) N. Kalva, N. Parekh, A. V. Ambade, *Polym. Chem.* **2015**, *6*, 6826-6835; (f) K. Ding, L. Shi, L. Zhang, T. Zeng, Y. Yin, Y. Yi, *Polym. Chem.* **2016**, *7*, 899-904.

[80] S. Z. Joshua S. Katz, Brendon G. Ricart, Darrin J. Pochan, Daniel A. Hammer and Jason A. Burdick, *J. Am. Chem Soc.* **2010**, *132*, 3654–3655

[81] H. Yang, L. Jia, Z. Wang, A. l. Di-Cicco, D. Lévy, P. Keller, *Macromolecules* **2011**, *44*, 159-165.

[82] M. Cao, J.-Q. Wang, P.-C. Chen, J.-T. Xu, Z.-Q. Fan, *J Polym Sci Part A: Polym Chem* **2010**, *48*, 3834-3840.

[83] J. Wang, Y. Ouyang, S. Li, X. Wang, Y. He, *RSC Adv.* **2016**, *6*, 57227-57231.

[84] N. G. Patil, N. B. Basutkar, A. V. Ambade, *Chem Commun (Camb)* **2015**, *51*, 17708-17711.

[85] C. Komeda, A. Ikeda, J. Kikuchi, N. Ishida-Kitagawa, H. Tatebe, K. Shiozaki, M. Akiyama, *Org Biomol Chem* **2013**, *11*, 2567-2570.

[86] D. Zhou, J. Guo, G. B. Kim, J. Li, X. Chen, J. Yang, Y. Huang, *Adv Healthc Mater* **2016**, *5*, 2493-2499.

[87] D. Tila, S. Ghasemi, S. N. Yazdani-Arazi, S. Ghanbarzadeh, *J Biomater Appl* **2015**, *30*, 3-16.

[88] F. D. Maria Laura Immordino, Luigi Cattel, *Int J Nanomedicine* **2006**, *1*, 297–315.

[89] H. R. Marsden, I. Tomatsu, A. Kros, *Chem Soc Rev* **2011**, *40*, 1572-1585.

[90] A. S. Janoff, *Lab Invest* **1992**, *66*, 655-658.

[91] S. Leekumjorn, H. J. Cho, Y. F. Wu, N. T. Wright, A. K. Sum, C. Chan, *Bba-Biomembranes* **2009**, *1788*, 1508-1516.

[92] M. M. Sperotto, O. G. Mouritsen, *Eur Biophys J Biophy* **1988**, *16*, 1-10.

[93] A. Samad, Y. Sultana, M. Aqil, *Curr Drug Deliv* **2007**, *4*, 297-305.

[94] M. L. Briuglia, C. Rotella, A. McFarlane, D. A. Lamprou, *Drug Deliv Transl Re* **2015**, *5*, 231-242.

[95] F. Versluis, J. Voskuhl, B. van Kolck, H. Zope, M. Bremmer, T. Albregtse, A. Kros, *J Am Chem Soc* **2013**, *135*, 8057-8062.

[96] J. S. Suk, Q. G. Xu, N. Kim, J. Hanes, L. M. Ensign, *Adv Drug Deliver Rev* **2016**, *99*, 28-51.

[97] J. Tang, L. Zhang, H. Gao, Y. Liu, Q. Zhang, R. Ran, Z. Zhang, Q. He, *Drug Deliv* **2016**, *23*, 1130-1143.

[98] B. Gupta, T. S. Levchenko, D. A. Mongayt, V. P. Torchilin, *J Drug Target* **2005**, *13*, 337-343.

[99] H. Brooks, B. Lebleu, E. Vives, *Adv Drug Deliver Rev* **2005**, *57*, 559-577.

[100] P. S. Kulkarni, M. K. Haldar, R. R. Nahire, P. Katti, A. H. Ambre, W. W. Muhonen, J. B. Shabb, S. K. Padi, R. K. Singh, P. P. Borowicz, D. K. Shrivastava, K. S. Katti, K. Reindl, B. Guo, S. Mallik, *Mol Pharm* **2014**, *11*, 2390-2399.

[101] G. Byk, C. Dubertret, V. Escriou, M. Frederic, G. Jaslin, R. Rangara, B. Pitard, J. Crouzet, P. Wils, B. Schwartz, D. Scherman, *J Medi Chem* **1998**, *41*, 224-235.

[102] H. Xu, Y. Deng, D. Chen, W. Hong, Y. Lu, X. Dong, *J Control Release* **2008**, *130*, 238-245.

[103] T. Wang, J. R. Upponi, V. P. Torchilin, *Int J Pharm* **2012**, *427*, 3-20.

[104] J. B. a. F. C. S. Harma Ellens, *Bichemistry* **1986**, *25*, 4141-4147.

[105] Y. Z. Wang, L. Chen, Y. F. Ding, W. L. Yan, *Int J Pharm* **2012**, *422*, 409-417.

[106] J. Miao, X. G. Zhang, Y. Hong, Y. F. Rao, Q. Li, X. J. Xie, J. E. Wo, M. W. Li, *Carbohyd Polym* **2012**, *87*, 1342-1347.

[107] S. M. Garg, I. M. Paiva, M. R. Vakili, R. Soudy, K. Agopsowicz, A. H. Soleimani, M. Hitt, K. Kaur, A. Lavasanifar, *Biomaterials* **2017**, *144*, 17-29.

[108] W. W. Xiao, N. Suby, K. Xiao, T. Y. Lin, N. Al Awwad, K. S. Lam, Y. P. Li, *J Control Release* **2017**, *264*, 169-179.

[109] J. N. Israelachvili, D. J. Mitchell, B. W. Ninham, *J Chem Soc Farad T 2* **1976**, *72*, 1525-1568.

[110] K. K. Gill, A. Kaddoumi, S. Nazzal, *J Drug Target* **2015**, *23*, 222-231.

[111] Z. Y. He, B. Y. Chu, X. W. Wei, J. Li, C. K. Edwards, 3rd, X. R. Song, G. He, Y. M. Xie, Y. Q. Wei, Z. Y. Qian, *Int J Pharm* **2014**, *469*, 168-178.

[112] C. Zhao, H. Deng, J. Xu, S. Li, L. Zhong, L. Shao, Y. Wu, X. J. Liang, *Nanoscale* **2016**, *8*, 10832-10842.

[113] Y. Lee, K. Kataoka, *Soft Matter* **2009**, *5*, 3810.

[114] K. M. Seiji Takae, Makoto Oba, Takehiko Ishii, Nobuhiro Nishiyama, Keiji Itaka, Yuichi Yamasaki, Hiroyuki Koyama and Kazunori Kataok, *J. Am. Chem. Soc.* **2008**, *130*, 6001–6009.

[115] Q. Tang, B. Cao, G. Cheng, *Chem Comm* **2014**, *50*, 1323-1325.

[116] (a) Y. Zhao, J. Zhao, C. Hao, M. Han, M. Wang, Y. Guo, X. Wang, *RSC Adv.* **2016**, *6*, 2602-2610; (b) X. Mao, J. Si, Q. Huang, X. Sun, Q. Zhang, Y. Shen, J. Tang, X. Liu, M. Sui, *Adv Healthc Mater* **2016**, *5*, 2517-2527; (c) P. F. Gou, W. W. Liu, W. W. Mao, J. B. Tang, Y. Q. Shen, M. H. Sui, *J Mater Chem B* **2013**, *1*, 284-292.

[117] (a) Q. Wu, F. Du, Y. Luo, W. Lu, J. Huang, J. Yu, S. Liu, *Colloids Surf B Biointerfaces* **2013**, *105*, 294-302; (b) A. Guiotto, M. Canevari, P. Orsolini, O. Lavanchy, C. Deuschel, N. Kaneda, A.

Kurita, T. Matsuzaki, T. Yaegashi, S. Sawada, F. M. Veronese, *Bioorg Med Chem Lett* **2004**, *14*, 1803-1805.

[118] K. Riebeseel, E. Biedermann, R. Loser, N. Breiter, R. Hanselmann, R. Mulhaupt, C. Unger, F. Kratz, *Bioconjug Chem* **2002**, *13*, 773-785.

[119] T. Liu, X. Yuan, T. Jia, C. Liu, Z. Ni, Z. Qin, Y. Yuan, *Int J Pharm* **2016**, *506*, 382-393.

[120] J. Lu, Y. Huang, W. Zhao, Y. Chen, J. Li, X. Gao, R. Venkataramanan, S. Li, *Mol Pharm* **2013**, *10*, 2880-2890.

[121] C. Li, L. Dai, K. Liu, L. Deng, T. Pei, J. Lei, *RSC Adv.* **2015**, *5*, 74828-74834.

[122] T. Yin, Q. Wu, L. Wang, L. Yin, J. Zhou, M. Huo, *Mol Pharm* **2015**, *12*, 3020-3031.

[123] (a) J. Lu, Y. Huang, W. Zhao, R. T. Marquez, X. Meng, J. Li, X. Gao, R. Venkataramanan, Z. Wang, S. Li, *Biomaterials* **2013**, *34*, 1591-1600; (b) Y. Huang, J. Lu, X. Gao, J. Li, W. Zhao, M. Sun, D. B. Stolz, R. Venkataramanan, L. C. Rohan, S. Li, *Bioconjug Chem* **2012**, *23*, 1443-1451.

[124] J. Liu, P. Zahedi, F. Zeng, C. Allen, *J Pharm Sci* **2008**, *97*, 3274-3290.

[125] (a) X. Zhang, K. Liu, Y. Huang, J. Xu, J. Li, X. Ma, S. Li, *Bioconjug Chem* **2014**, *25*, 1689-1696; (b) X. Zhang, Y. Huang, M. Ghazwani, P. Zhang, J. Li, S. H. Thorne, S. Li, *ACS Macro Letters* **2015**, *4*, 620-623; (c) X. Zhang, J. Lu, Y. Huang, W. Zhao, Y. Chen, J. Li, X. Gao, R. Venkataramanan, M. Sun, D. B. Stolz, L. Zhang, S. Li, *Bioconjug Chem* **2013**, *24*, 464-472; (d) X. Zhang, Y. Huang, W. Zhao, Y. Chen, P. Zhang, J. Li, R. Venkataramanan, S. Li, *Mol Pharm* **2014**, *11*, 2807-2814; (e) Y. Chen, X. Zhang, J. Lu, Y. Huang, J. Li, S. Li, *AAPS J* **2014**, *16*, 600-608.

[126] H. Wang, J. He, D. Cao, M. Zhang, F. Li, K. C. Tam, P. Ni, *Polym. Chem.* **2015**, *6*, 4809-4818.

[127] (a) S. Yang, F. Zhu, Q. Wang, F. Liang, X. Qu, Z. Gan, Z. Yang, *J. Mater. Chem. B* **2015**, *3*, 4043-4051; (b) G. Salzano, D. F. Costa, C. Sarisozen, E. Luther, G. Mattheolabakis, P. P. Dhargalkar, V. P. Torchilin, *Small* **2016**, *12*, 4837-4848.

[128] Z. Dai, Y. Tu, L. Zhu, *J Biomed Nanotechnol* **2016**, *12*, 1199-1210.

[129] D. E. Discher, F. Ahmed, *Annu Rev Biomed Eng* **2006**, *8*, 323-341.

[130] M.-H. Li, P. Keller, *Soft Matter* **2009**, *5*, 927.

[131] L. Messager, J. Gaitzsch, L. Chierico, G. Battaglia, *Curr Opin Pharmacol* **2014**, *18*, 104-111.

[132] D. V. Simona Cerritelli, and Jeffrey A. Hubbell, *Biomacromolecules,* **2007**, *8*, 1966-1972.

[133] T. Thambi, V. G. Deepagan, H. Ko, D. S. Lee, J. H. Park, *J Mater Chem* **2012**, *22*, 22028.